

1 Dear Editor,

2  
3 Please find attached our revised manuscript for publication in Climate of the Past.

4 We addressed all reviewers points as specified in the online discussion, and provide  
5 here a stronger manuscript. More specifically, amongst the different points we  
6 addressed issues making reviewer #3 ask for major revisions :

7 -Validation of our model with data (this point was also raised by rev#2): We  
8 did the analyses recommended by Rev#3 and showed that the latitudinal isotopic  
9 gradient was well-represented by LMDZ-iso and that despite some model-data  
10 mismatches (that are now discussed), modeled vs. observed values gives a good fit.

11 - Explanation of the decomposition methods: We have rewritten the methods  
12 section to be clearer. Explanations for equations are more detailed.

13 - Robustness of the methods : We benefited a lot from rev#3 comments and  
14 rewrote our equations to provide a more robust decomposition. Following rev#3  
15 suggestions, we have (1) weighted our decomposition terms by rainfall amount, (2)  
16 checked the sensitivity to initial values, (3) checked the sensitivity to the state at  
17 which the decomposition terms have been calculated, by using a new decomposition  
18 method, based on centered differences.

19  
20 Sincerely,

21 The authors.  
22  
23  
24  
25  
26  
27  
28  
29  
30  
31  
32  
33

## Response to anonymous review #1

We thank anonymous reviewer #1 for these comments. Indeed, we present simulations with two cases of the Tibetan Plateau elevation ( $\frac{1}{2}$  of current topography and reduced to 250 m topography over the region) with a purpose of testing the sensitivity of  $\delta^{18}\text{O}$  to the topography change. Zoomed experiments including the isotopes are very expensive in terms of computation time (about 700 days of single CPU core time per experiment) and it is technically difficult to test multiple elevation scenarios. We suggest that the end-members of elevation scenarios (MOD and LOW) and the middle case (INT) are good representative of the spectrum of altitude/ $\delta^{18}\text{O}$  relationships. We assume that any additional scenarios with more detailed steps of relief variations would provide more information regarding altitudinal values (and possible threshold) affecting atmospheric dynamics. Still it would not change our main conclusions, i.e. that the isotopic composition of precipitation is very sensitive to climate changes related.

## Response to anonymous review #2

We thank the Anonymous Referee #2 for this constructive review. We will provide the editor and reviewers with a corrected manuscript, meanwhile here is a point-by-point response:

(a) Model validation is obviously very important. First of all, we want to stress that LMDZ has been used for numerous present-day climate and paleoclimate studies (Kageyama et al., 2005; Ladant et al., 2014; Sepulchre et al., 2006), including studies of monsoon region (eg. (Lee et al., 2012; Licht et al., 2014). Yao et al., [2013] also showed that LMDZ-iso has the best representation of the altitudinal effect compared to other GCM and RCM isotope-equipped models. These authors also have provided a detailed description of rainfall patterns over the Tibetan Plateau, and showed LMDZ-iso ability to simulate atmospheric dynamics and reproduce rainfall and  $\delta^{18}\text{O}$  patterns consistent with data over this region. For the purpose of our experiments validation, in the current manuscript version we compare MOD run outputs with rainfall data from the Climate Research Unit (CRU) (New et al., 2002). Corresponding figure is in the supplementary materials (Fig. S1). When compared to

CRU dataset, MOD annual rainfalls depict an overestimation over the high topography of the Himalayas and the southern edge of the Plateau, with a rainy season, which starts too early and ends too late in the year. Over central Tibet (30-35°N), the seasonal cycle is well captured by LMDz-iso, although monthly rainfall is always slightly overestimated (+0.5 mm/day). CRU data shows that the northern TP (35-40°N) is dryer with no marked rainfall season and a mean rainfall rate of 0.5 mm/day. In MOD experiment, this rate is overestimated (1.5 mm/day on annual average). In addition, we suggest to provide a comparison of humidity transport between LMDZ-iso MOD simulation outputs and ERA-40 re-analysis data (Uppala et al., 2005). This comparison depicts reasonable representation of both directions and magnitudes of moisture transport patterns by LMDZ-iso model. Model slightly overestimates the moisture transport magnitude to the west and north of the TP. Despite some model-data mismatches, the ability of LMDZ-iso to represent the seasonal cycle in the south and the rainfall latitudinal gradient over the TP as well as reasonable humidity transport allows its use for the purpose of this study. To make this comparison clearer, we will add these explanations in the corrected manuscript text and add an extra figure with model-data (with CRU precipitation) comparison to the main text and add an additions panel to the Fig. 4 with humidity transport from the ERA-40 re-analysis data.

- (b) The reviewer raises a very important point. First of all, for each modelling study there are limitations associated with experimental design. In this study the topography uplift scenarios are clearly idealized, as our purpose is to test the sensitivity of  $\delta^{18}\text{O}$  to the climatic changes associated with the topography uplift. For a purpose of using GCM simulations as “forward proxy modelling” (Sturm et al., 2010), realistic experiments should be designed, including accurate paleo  $\text{pCO}_2$ , land-sea distribution and latitudinal positions of continents. On the other hand, as it was noted by Anonymous Referee #2,  $\delta^{18}\text{O}$  distribution is highly dependant of hydrological cycle representation in GCM simulations. Comparing the simulated and observed precipitation and humidity transport in the new figures, some model-data mismatches are identified. Model-data comparison show that mean annual precipitation amount is slightly overestimated by the model for the northern TP, thus could result in underestimation of the amount effect contribution for the northern TP. On the contrary precipitation model overestimates the precipitation over the southern edge of

Himalayas. If it was more realistic, the contribution of the amount effect estimated by the decomposing method would be less important. We will add a paragraph discussing these uncertainties in the conclusion section of the corrected manuscript.

(c) The difference between  $\delta^{18}\text{O}_{\text{vapour}}$  and  $\delta^{18}\text{O}_{\text{precipitation}}$  is linked to the post-condensation effects, mainly associated with raindrop reevaporation that can occur after initial condensation. Because lighter isotopes evaporate more easily, rain reevaporation leads to an isotopic enrichment of precipitation. Therefore, the more reevaporation, the greater the difference between  $\delta^{18}\text{O}_{\text{precipitation}}$  and  $\delta^{18}\text{O}_{\text{vapour}}$ . We will explain this better in the paper. We refer to the study of (Lee and Fung, 2008), where post-condensation effects are explained in details. The contribution of such processes increases dramatically for very dry areas, where the relative humidity is less than 40%. In the absence of the TP (LOW experiment), large-scale subsidence superimposed to the sea surface pressure low anomaly (“Thermal Low”) induces very dry condition over Asia (Fig. S2) which are favourable for high rate of post-condensational effects (Fig. 8). In contrast, the HTP uplift even to the INT height cancels the Thermal Low structure and creates relatively wet conditions (the relative humidity > 40%) over HTP with raindrop reevaporation playing a secondary role. Aridification of the Tarim Basin and creation of Taklimakan desert that is simulated for the MOD case makes post-condensational effects important over this region for the second uplift stage (Fig. 9). We agree that it is necessary to make this point clearly in the corrected manuscript.

(d) , (e) Thank you that you noticed this issue, we will change the order of figures and do necessary corrections.

Kageyama, M., Nebout, N. C., Sepulchre, P., Peyron, O., Krinner, G., Ramstein, G. and Cazet, J.-P.: The Last Glacial Maximum and Heinrich Event 1 in terms of climate and vegetation around the Alboran Sea: a preliminary model-data comparison, *Comptes Rendus Geosci.*, 337(10-11), 983–992, doi:10.1016/j.crte.2005.04.012, 2005.

Ladant, J., Donnadiou, Y., Lefebvre, V. and Dumas, C.: The respective role of atmospheric carbon dioxide and orbital parameters on ice sheet evolution at the Eocene-Oligocene transition, *Paleoceanography*, 29(8), 810–823, doi:10.1002/2013PA002593, 2014.



1 Lee, J. and Fung, I.: “Amount effect” of water isotopes and quantitative analysis of post-  
2 condensation processes, *Hydrol. Process.*, 22(1), 1–8, 2008.

3 Lee, J. E., Risi, C., Fung, I., Worden, J., Scheepmaker, R. A., Lintner, B. and  
4 Frankenberg, C.: Asian monsoon hydrometeorology from TES and SCIAMACHY water  
5 vapor isotope measurements and LMDZ simulations: Implications for speleothem climate  
6 record interpretation, *J. Geophys. Res. Atmos.*, 117(15), 1–12,  
7 doi:10.1029/2011JD017133, 2012.

8 Licht, A., van Cappelle, M., Abels, H. A., Ladant, J.-B., Trabucho-Alexandre, J., France-  
9 Lanord, C., Donnadieu, Y., Vandenberghe, J., Rigaudier, T., Lécuyer, C., Terry Jr, D.,  
10 Adriaens, R., Boura, A., Guo, Z., Soe, A. N., Quade, J., Dupont-Nivet, G. and Jaeger, J.-  
11 J.: Asian monsoons in a late Eocene greenhouse world, *Nature*, 513(7519), 501–506,  
12 doi:10.1038/nature13704, 2014.

13 New, M., Lister, D., Hulme, M. and Makin, I.: A high-resolution data set of surface  
14 climate over global land areas, *Clim. Res.*, 21(1), 1–25, doi:10.3354/cr021001, 2002.

15 Sepulchre, P., Ramstein, G., Fluteau, F., Schuster, M., Tiercelin, J.-J. and Brunet, M.:  
16 Tectonic uplift and Eastern Africa aridification., *Science*, 313(5792), 1419–1423,  
17 doi:10.1126/science.1129158, 2006.

18 Sturm, C., Zhang, Q. and Noone, D.: An introduction to stable water isotopes in climate  
19 models: benefits of forward proxy modelling for paleoclimatology, *Clim. Past*, 6(1), 115–  
20 129, 2010.

21 Uppala, S. M., Kållberg, P. W., Simmons, A. J., Andrae, U., Bechtold, V. D. C., Fiorino,  
22 M., Gibson, J. K., Haseler, J., Hernandez, A., Kelly, G. A., Li, X., Onogi, K., Saarinen,  
23 S., Sokka, N., Allan, R. P., Andersson, E., Arpe, K., Balmaseda, M. A., Beljaars, A. C.  
24 M., Berg, L. Van De, Bidlot, J., Bormann, N., Caires, S., Chevallier, F., Dethof, A.,  
25 Dragosavac, M., Fisher, M., Fuentes, M., Hagemann, S., Hólm, E., Hoskins, B. J.,  
26 Isaksen, I., Janssen, P. A. E. M., Jenne, R., McNally, A. P., Mahfouf, J.-F., Morcrette, J.-  
27 J., Rayner, N. A., Saunders, R. W., Simon, P., Sterl, A., Trenberth, K. E., Untch, A.,  
28 Vasiljevic, D., Viterbo, P. and Woollen, J.: The ERA-40 re-analysis, *Q. J. R. Meteorol.*  
29 *Soc.*, 131(612), 2961–3012, doi:10.1256/qj.04.176, 2005.

30 Yao, T., Masson-Delmotte, V., Gao, J., Yu, W., Yang, X., Risi, C., Sturm, C., Werner,  
31 M., Zhao, H., He, Y., Ren, W., Tian, L., Shi, C. and Hou, S.: A review of climatic  
32 controls on  $\delta^{18}\text{O}$  in precipitation over the Tibetan Plateau: Observations and simulations,  
33 *Rev. Geophys.*, 51(4), 525–548, doi:10.1002/rog.20023, 2013.

**Point by point reply to the comments from Anonymous Referee #3**

**R3:** *“This manuscript uses an isotope-enabled GCM to understand how the many factors that influence rainfall isotopes shape the  $\delta^{18}\text{O}$  of rainfall in the Himalaya-Tibet Plateau (HTP) region as topography changes. This is the first manuscript I have seen examining this topic in the HTP region although other papers have used a similar approach in S. America and elsewhere. This is an important topic to understand as it underpins the field of isotope paleoaltimetry and inferences of the topographic history of the HTP region. The paper is well written and informative, especially the author’s decomposition of the isotope changes into different processes.”*

A: We thank Anonymous Referee #3 for this appreciation of our work.

**R3:** *“The major comments I have relate to the mismatch between the modern and model  $\delta^{18}\text{O}$  gradients on Tibet and the details of the decomposition method. I recommend acceptance after major revisions. I think the fundamental study and analysis approach is sound. However, additional explanation of the methodology and exploration of the limitations of the model are needed to make the paper useful to readers. I am also not sure their analysis will end with the same conclusions if different methods for decomposing the isotope signal are used (precip weighting climate values, non-linear adiabats that change with temperature etc.).”*

A: We thank the Anonymous Referee #3 for this very constructive review. We will provide all necessary correction in the corrected manuscript version. Meanwhile, for the online discussion, we provide a detailed point-by-point response and a reworked methods section in the end of this document.

**Response to Major comments:**

**R3:** *“1. The methods for decomposing the rainfall isotope change into different components was difficult to follow. Additional details would greatly help the reader understand this process. I have a few specific notes about this below but encourage a more general re-thinking of this explanation to make it explicit how each of the terms are derived (particularly the partial differentials, reference values  $R_{vo}$ ,  $T_o$  etc.).”*

**A:** Thank you, we agree that the theoretical framework for the precipitation decomposition method has to be better explained. In the revised version of the manuscript we rewrite the method part with a purpose to make it clearer for readers. Full rewriting of section 2.3 is underway to make clear how each term is calculated. You will find a reworked version of sections “1. Theoretical framework for the precipitation composition” and “2. Decomposition of precipitation composition differences” below point-by-point response. We will remove the partial differentials, because it is misleading. We don't calculate partial differentials, we calculate total differences. How each term is calculated as a difference will be explicated.

**R3:** “1a. It is not directly clear how the different processes that contribute to rainfall isotope change are actually calculated. For example, how is  $dR_{vi}$  (Eq 3) actually calculated? What region is used to define  $R_{vi}$  and  $R_{vo}$  so as to calculate  $dR_{vi}$ ? Likewise, where is  $q_0$  determined (eq 4),  $T_0$  (eq. 6) etc. A much more detailed explanation is needed I think. How is the change in elevation contribution to rainfall isotopes calculated (it depends upon  $dz$  times lapse rate but also depends upon the Rayleigh distillation, saturation relationship to  $T$ ). What is the actual analytical term for the partial differential in Eq. 8?”

**A:** We add more detailed explanations and a specific equation for each analytical term from the Eq. 8 (see the end of this document). We assume that the  $\delta R_{vi}$  term is a residual part of the vapor isotopic difference that accounts for processes of deep convection and air mass mixing. Equations from section 2 (see the decomposition method below point-by-point response) show that we do not need to know  $\delta R_{vi}$  to estimate its contribution to the total isotopic change between two cases. For parameters  $z_0$ ,  $q_0$  and  $T_0$  we took values over New Delhi region to be consistent with previous isotopic studies over the region, but the sensitivity to these arbitrary choices will be tested. Even if initial conditions for the Rayleigh distillation vary depending on the atmospheric circulation, on deep convective processes and on the site of interest, we keep the same reference values, and all variations in initial conditions are accommodated by  $\delta R_{vi}$ .

**R3:** “1b. Furthermore, it is not abundantly clear how the partial differentials in eq. 8 were evaluated. For example,  $dR_p/dR_{vi}$  (1<sup>st</sup> partial differential in Eq. 8) depends upon  $f$ , etc. (e.g. change in rainfall  $R_p$  depends upon initial vapor composition plus modification by isotope fractionation, the magnitude in per-mil also depends upon the initial vapor

composition). All of these partial differentials need to be more explicitly evaluated analytically in the paper and the dependence on the sensitivity of the partial differentials to the state at which they are calculated has to be demonstrated as not a factor (as is assumed on p7 L5).”

**A:** To make the decomposition processes clearer we address the reviewer to the reworked methodological part (see below point-by-point response), in which we added supplemental information and equations describing the evaluation of the five partial differentials.

We carried sensitivity tests for partial differentials: results are presented in two additional tables for the southern and northern regions (Tabl. 1 and Tabl. 2). The sensitivity to  $Rv0$  will remain as a multiplying factor. In addition, in the new version we will provide a test of the sensitivity of decomposition terms to the state at which they are calculated.

	Northern Region			South region		
	T0	Rh0	Rv0	T0	Rh0	Rv0
$\Delta R_{p,\Delta z}$	0,15	0,33	0,667	0,12	0,25	0,51
$\Delta R_{p,\Delta \delta T_s}$	0,09	0,02	0,04	0,12	0,06	0,13
$\Delta R_{p,\Delta h}$	0	0,351	0,66	0	0,19	0,83
$\Delta R_{p,\Delta \delta R_{vi}}$	0	0	0,05	0	0	0,52
$\Delta R_{p,\Delta \varepsilon}$	0	0	0	0	0	0

Tabl. 1. INT-LOW Sensitivity of the decomposition terms (in ‰) to the change of 1°C of T0 and 10 ‰ of Rh0 and 1 ‰ of Rv0.

	Northern Region			South region		
	T0	Rh0	Rv0	T0	Rh0	Rv0
$\Delta R_{p,\Delta z}$	0,36	0,6	1,4	0,3	0,59	1,2
$\Delta R_{p,\Delta \delta T_s}$	0,34	0,09	0,18	0,31	0,02	0,05

$\Delta R_{p,\Delta h}$	0	0,78	0,9	0	0,57	0,47
$\Delta R_{p,\Delta \delta R_{vi}}$	0	0	0,85	0	0	0,67
$\Delta R_{p,\Delta \varepsilon}$	0	0	0	0	0	0

Tabl. 2. MOD-INT Sensitivity of the decomposition terms (in ‰) to the change of 1° of T0, 0,1 of Rh0, 1 ‰ of Rv0

**R3:** “1c. Decomposition of the absolute humidity term into temperature and relative humidity means that attribution of  $\delta^{18}O$  changes to  $T_s$  or  $rh$  changes depends upon how well the model really captures those two values.”

**A:** We fully agree. The question of model validation has been also raised by the Anonymous reviewer #2. In the current manuscript version we compare MOD run outputs with rainfall data from the Climate Research Unit (CRU) [New *et al.*, 2002]. Corresponding figure is in the supplementary (Fig. S1). Also following reviewers recommendations we have added a comparison of humidity transport between LMDZ-iso MOD simulation outputs and ERA-40 re-analysis data [Uppala *et al.*, 2005]. Our MOD simulation is preindustrial, consequently a comparison with modern data is expected to provide differences driven by the pre-industrial boundary conditions. Still comparing LMDZ-iso outputs with mean annual temperatures from CRU dataset [New *et al.*, 2002] (Fig. N1) and relative humidity from NCEP-DOE Reanalysis. Fig. N2 shows that LMDZ-iso model captures these variables reasonably well.

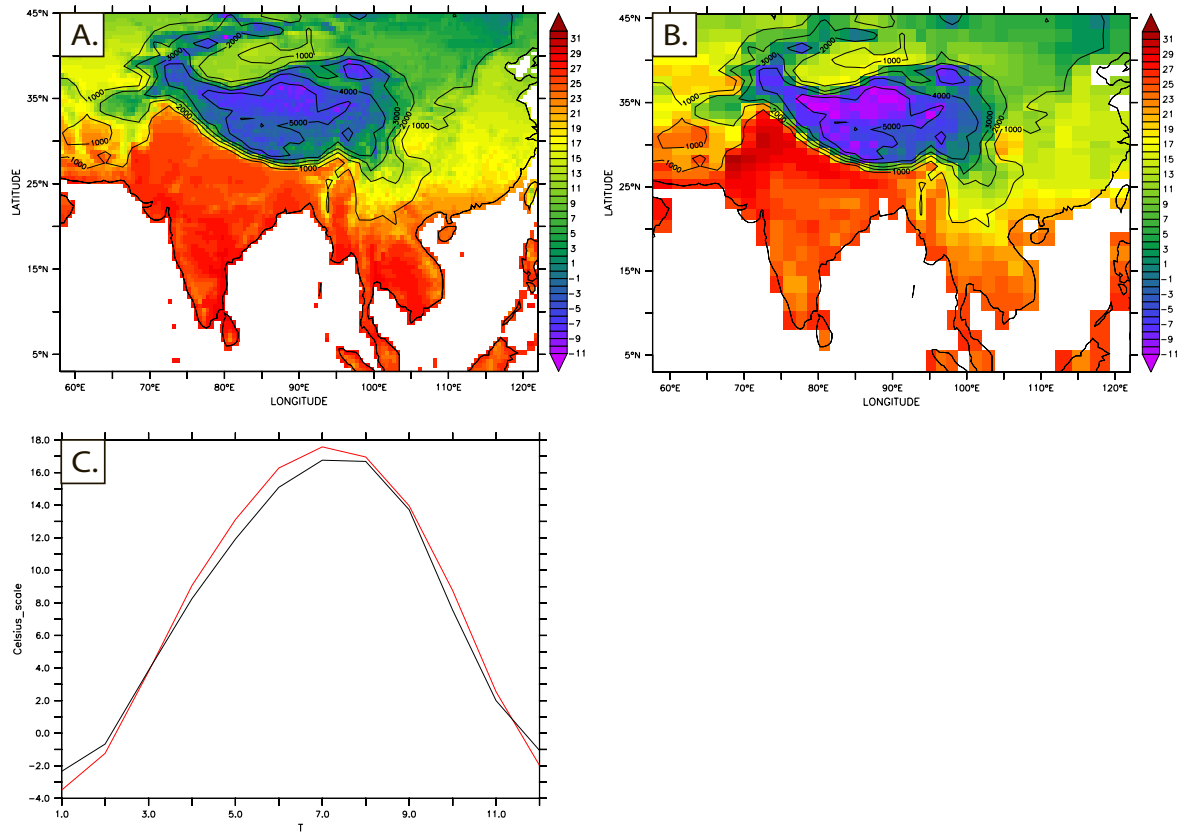


Fig. N1. Mean annual temperature from A) the Climate Research Unit (CRU) [New *et al.*, 2002] dataset and B) LMDZ-iso simulated for the MOD experiment. Figure (C) represent the seasonal cycles of temperature spatially averaged from 25°N to 40°N and from 70°E to 110°E for the MOD experiment (black) and for the CRU dataset (red).

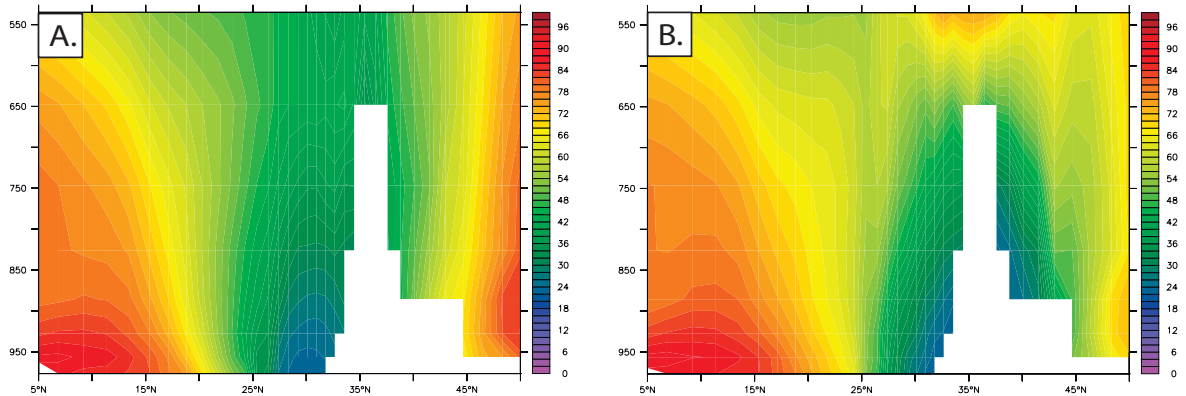


Fig. N2. Mean annual relative humidity profiles for A) NCEP-DOE Reanalysis and B) LMDZ-iso simulated for the MOD experiment.

**R3:** “Another, and more fundamental way to partition the rainfall  $\delta^{18}\text{O}$  changes would be to determine how much the specific humidity changes (or  $T^*$ ) contribute to the isotope

changes. This gets at the transport and rainout process more directly. The local  $T$  and  $rh$  values are not really the source of the isotope changes,  $T^*$  or  $q/q_0$  ( $q[T^*]/q_0$ ) are the actual cause of the changes (e.g. eq. 4). I would much rather the authors use  $T^*$  or  $q/q_0$  changes in their decomposition of the isotope changes (or at least do this in parallel to the  $T$ ,  $rh$  decomposition as they are equivalent). In equation 8 this would combine the  $Dh$  and  $DdT_s$  terms into a single  $q$  or  $T^*$  term. Intuitively this makes more sense:  $R_p$  is a function of  $R_{vi}$ ,  $\epsilon$ , and  $q$ .”

**A:** One of the main purposes of the paper is to estimate the value of the  $\frac{\partial R_p}{\partial z} \cdot \Delta z$  term. Altitude acts through temperature, this is why we chose to extract the temperature signal. We suggest to add an addition panel to the Fig. 8 and Fig. 9 that shows the part of the isotopic signal associated with the part of the change of the specific humidity with the uplift that is not associated with elevation (here Fig. N3). Nevertheless, we insist to keep all terms in the equation 8 as discussed below.

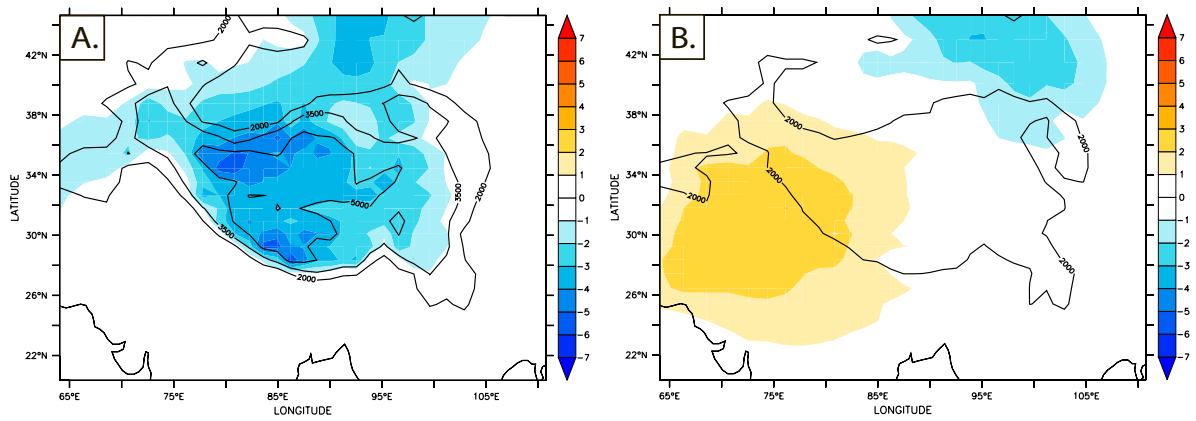


Fig. N3. The effect of specific humidity change

**R3:** “1d. The  $dz$  term in Eq. 8 is really a temperature change (or  $T^*$  change as is assumed in a Rowley type model - actually a Pierrehumbert-type model: Pierrehumbert, 1999 Huascaran  $d18O$  as an indicator of tropical climate during the Last Glacial Maximum). So, the  $q$  term could be decomposed into an elevation term and a non-elevation term. This would still keep the decomposition focused on the fundamental  $q/q_0$  term rather than  $T_s$  and  $rh$ .”

**A:** Our model is equivalent to that of Rowley et al (2001) for  $\delta R_{vi} = 0$  (i.e. neglecting the effects of mixing and deep convection on the initial water vapor),  $\epsilon = (a - 1) \cdot R_v$  (i.e. neglecting post-condensational effects), and  $h=1$  (i.e. assuming the site of interest is inside the precipitating cloud). We agree that the most important point of the paper is the

1 division of the total isotopic signal into an “elevation” and “non-elevation” term.  
2 However, we think that the relative humidity component is important from a physical  
3 point of view because it reflects the large-scale circulation: how high did the last  
4 saturation occur? Is the regime under large-scale ascent or descent? Actually we are  
5 showing an elevation term on Fig. 8 B and Fig. 9 B according to the uplift stage and non-  
6 elevation terms of Fig. 10 A and Fig. 11 A.

7  
8 **R3:** *“I.e. Are the values used to decompose the rainfall isotope changes precipitation*  
9 *weighted? That is, are  $q$ ,  $T$  etc. weighted by the precipitation amount in a particular*  
10 *location? One of the reasons that there is such a strong relationship between isotopes*  
11 *and elevation is that the relationship is set only when it rains. This is a very small subset*  
12 *of all atmospheric conditions and thus much of the variability really doesn’t matter. It*  
13 *only matters if it is actually raining and the isotope signal is being “sampled.” In my*  
14 *opinion, rainfall weighted climate variables are essential for properly decomposing the*  
15 *isotope signal.”*

16 **A:** In our calculations only  $\delta^{18}\text{O}$  values are weighted by the precipitation amount, but the  
17 climatic variables are not weighted. We have now recalculated all contributions using  
18 precipitation-weighted variables. In doing so, we used monthly outputs, so that the effects  
19 of seasonality are taken into account by the precipitation weighting. However, we do not  
20 have the daily outputs. So the effects of precipitation intermittency at the daily time scale  
21 won't be taken into account. We will acknowledge this limitation in the revised  
22 manuscript. Also, we checked that the decomposition terms calculated for the summer  
23 period with a large number of days when it rains is not essentially different from those  
24 calculated using mean annual values (fig. N4)



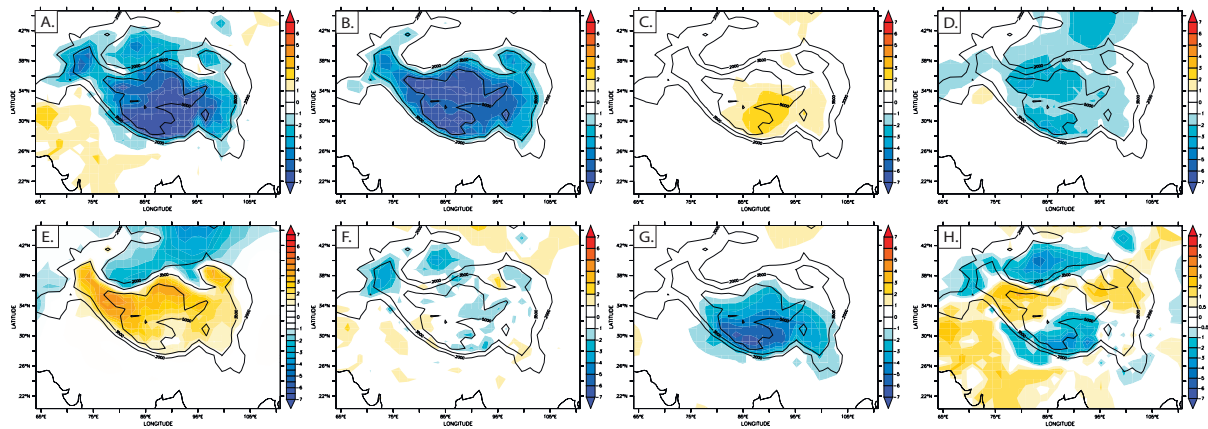


Fig N4. MJJAS total isotopic difference between MOD and INT experiments ( $\Delta R_p$ ) and spatial isotopic variations related to: (B) direct effect of topography changes, (C) effect of lapse rate change, associated with non-adiabatic effects, (D) effect of specific humidity, (E) effect of local relative humidity change, (F) effect of changes in post-condensational processes, (G) all other effect, (H) difference in  $\delta^{18}O_p$  between MOD and INT experiments that is not related to direct effect of topography changes

**R3:** “2. I think there are major and important differences in the modeled and observed rainfall isotopes (e.g. Fig. 7). This is particularly true for the northern plateau where isotope values in rainfall become so positive that they are nearly identical to low elevation rainfall south of the Himalaya. I disagree with the author’s statement that these highly enriched isotope values are from surface processes (p9 116-20). Bershaw et al, 2012 were discussing the Pamir region to the west and even in their data there is not evidence of non-equilibrium fractionation as would be expected from kinetic effects. Overall there is not a strong d- excess signal on the plateau as would be expected for evaporative processes thus the data indicate a robust positive isotope signal in rainfall values.”

**A:** We agree with the reviewer that over the northern part of the Plateau there are some model-data discrepancies that could not be explained by the surface processes. On the contrary, we would like to pay attention on the very good model-data fit of isotopic data over the northern-east slope of the TP (Bershaw et al., 2011). Over the northern margins of the TP, modelled  $\delta^{18}O$  in precipitation is more negative than observations show. This model-data discrepancies may result from 3 types of uncertainties: 1) linked with the

1 model resolution. Despite quite a high resolution that we are able to obtain with a zoomed  
2 grid, the relief could be not represented well at some parts of the TP, and 2)  
3 overestimation by the model of the westerlies flux (see the comparison with the ERA  
4 moisture transport) that probably lead to underestimation of  $\delta^{18}\text{O}$  over the northern part  
5 of the TP. Our statement about the contribution of the surface processes to more positive  
6 values over the central part (p9 116-20) of the TP (data of Quade) is consistent with the  
7 Quade explanation of the increased role of the continental recycling northward from the  
8 Himalayas crest.

9  
10 **R3:** *“This feature, its interpretation, and whether and why it persists in the past are*  
11 *perhaps some of the major questions in Tibetan paleoaltimetry. If it is a persistent feature*  
12 *then ancient isotope values from central and northern Tibet that look like today’s values*  
13 *may have come from modern-like elevations. If this is not a persistent feature (e.g. an*  
14 *arm of the Tethys north of Tibet would provide local moisture) then ancient isotope*  
15 *values that are the same as today may actually mean the site was at a low elevation.”*

16 **A:** We agree. In this paper we provide only sensitivity experiments with reduced  
17 topography. The influence of realistic paleogeography (eg. with the Tethys Sea, altered  
18 paleogeography) on the isotopic composition of precipitation is a topic of our further  
19 studies. However, the reviewer’s point is very important and we discuss the possible  
20 sources of uncertainties while comparison with deep paleo data and further studies  
21 directions on p18 17-10.

22  
23 **R3:** *“My recommendations for this issue are twofold. First, I would like to see two*  
24 *scatterplots in addition to the heat map. The first would be the observed vs. modeled  $\delta^{18}\text{O}$*   
25 *rainfall from Fig. 7A along with RMSE estimates. This plot would show how well the*  
26 *model really captures isotope values regardless of location. The second would have*  
27 *latitude as an x-axis and actual observations of oxygen isotope values as the y axis along*  
28 *with values from the model as a continuous line. Values could be from a swath beginning*  
29 *at the south and extending north along the central axis of the plateau or projected in from*  
30 *the plateau. This plot would show how well the model gets the overall isotope gradient*  
31 *even if it doesn’t get the absolute values correctly.*  
32 *Second would be a thorough discussion of what this mismatch means for interpretation of*  
33 *the model experiments. If the model is missing or underrepresents some moisture source*

or process that is important today on the northern plateau then what does this mean for the conclusions from the model experiments?"

**A:** Thank you for this recommendation. On the Fig. N5 observed vs. modeled  $\delta^{18}\text{O}$  rainfall scatter plot is presented with a linear regression. Modeled vs observed data show quite a good correlation with a Pearson coefficient of 0,8646. Fig N6 shows a map of modeled  $\delta^{18}\text{O}$  for the MOD experiment overplotted by observed data values and a south-north transection (averaged between 70 and 100° E) of modelled values (black line) and projected in observed values of  $\delta^{18}\text{O}$ . The general south-north isotopic gradient is simulated perfectly well by the model. After the Himalayan crest  $\delta^{18}\text{O}_p$  values become more positive that is consistent with a South-North trend observed by Quade et al. [Quade et al., 2007; Bershaw et al., 2012b].

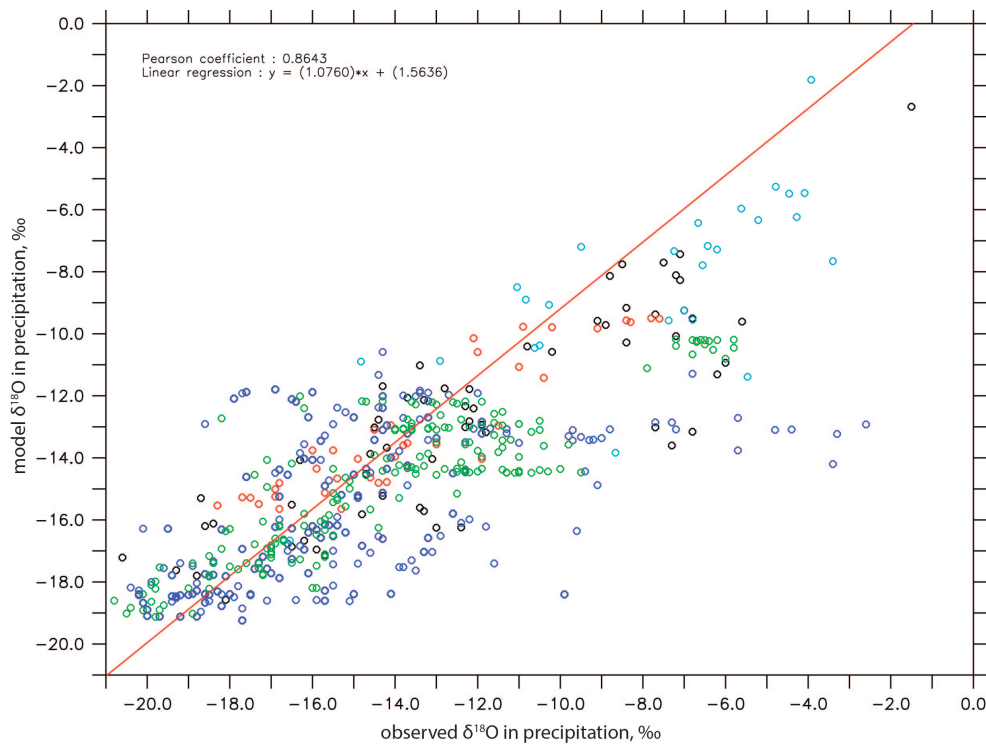


Fig. N5. Model vs observed  $\delta^{18}\text{O}$  in precipitation. The colour of circles corresponds to the data set: red – Bershaw et al, 2012, blue – Quade et al, 2011, green – Hren et al, 2009, black – Caves et al, 2015, light blue show mean annual data from GNIP stations. Red line shows a linear regression.

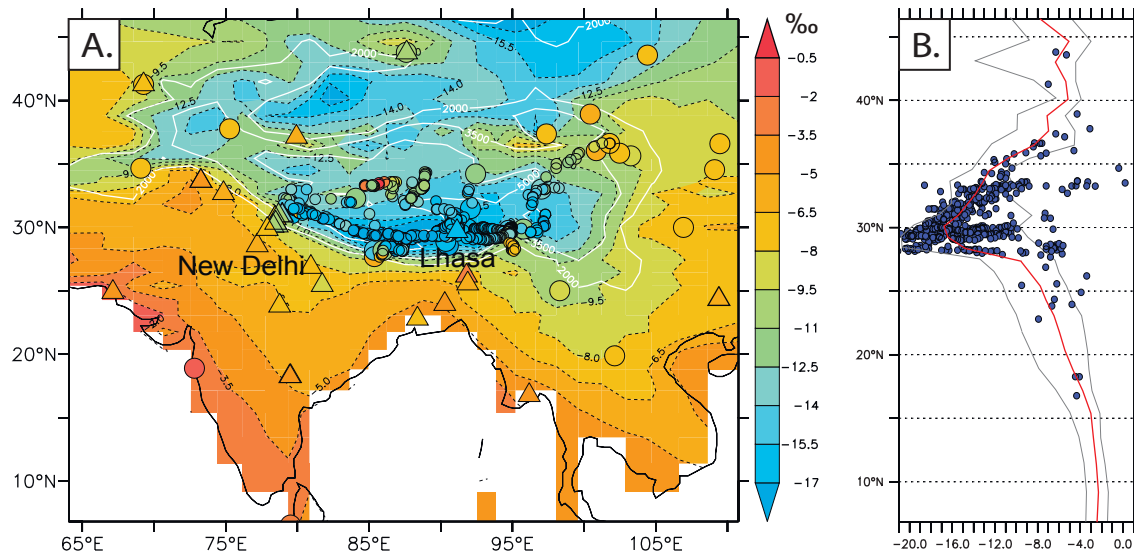


Fig. N6. A) Annual mean  $\delta^{18}\text{O}$  in precipitation simulated by LMDZ-iso for the MOD case and B) S-N profiles of model simulated  $\delta^{18}\text{O}$  in precipitation for the MOD case. Points correspond to present-day  $\delta^{18}\text{O}$  from published data (Bershaw et al, 2012, Quade et al, 2011, Hren et al, 2009, Caves et al, 2015), and mean annual data from GNIP stations). Solid black line shows model  $\delta^{18}\text{O}$  values averaged between  $70^\circ\text{E}$  and  $100^\circ\text{E}$ . Grey lines show minimum and maximum values for the selected range of longitudes.

**R3:** “3. Cite the original sources for precipitation isotope values on the plateau. These authors should get credit for the major amount of work it takes to generate this type of data and all the credit shouldn’t go to the Caves 2015 compilation.”

**A:** Thank you for this remark. We have added the references to the original papers.

**R3:** “One of the major conclusions of the paper is that there is a non-linear effect of elevation changes on isotope values. One expects a non-linear relationship between rainfall isotope values and elevation simply because of the non-linearity of (i) saturated adiabats, (ii) the saturation vapor pressure curve with temperature and (iii) the Rayleigh distillation process itself. Thus the null hypothesis is that isotope changes with elevation from low to intermediate elevations would be less than isotope changes from intermediate to high elevations. Whether the changes are greater than can be explained by the null hypothesis needs to be demonstrated. But, the qualitative observation itself is actually expected from theory. An additional plot would drive this home. What does a Rowley (Pierrehumbert) type model predict for isotope change with elevation and where do these GCM models plot? I would focus this plot on the Himalayan mountain region as this is

where the simple model is most applicable. This would be an incredibly useful plot for folks that want to take lessons away from this paper. How similar/different are the results in this paper from a simple model that has been extensively used to reconstruct elevation?”

**A:** We agree with the reviewer that our conclusion about non-linearity of the magnitude of the isotopic changes between the initial and the terminal stage of the uplift is a logical consequence of non-linearity of saturated adiabats, the saturation vapour pressure curve with temperature and the Rayleigh distillation process. However we find useful to stress this interesting characteristic for the geological community since such a conclusion has never been published before. The estimation whether the changes are greater than can be explained by the null hypothesis is out of scope of the paper and may be a subject of another study. Here we suggest an additional figure (Fig. N7) showing  $\Delta(\delta^{18}\text{O})$  vs elevation for MOD and INT simulations and Rowley type model (Rowley et al., 2001).

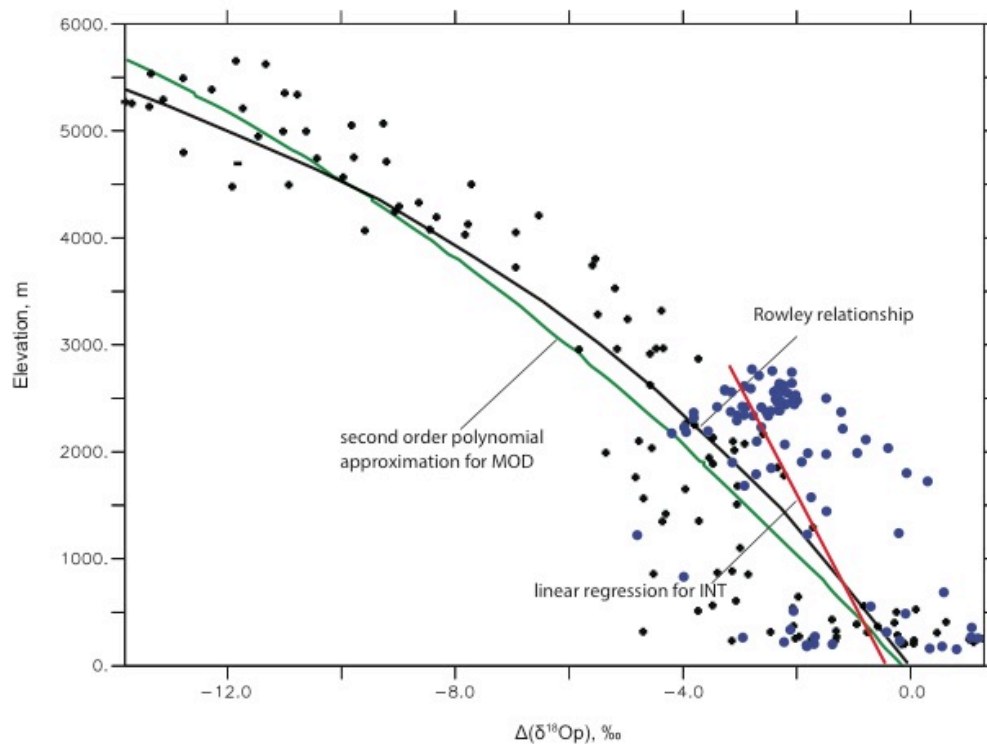


Fig. N7.  $\Delta(\delta^{18}\text{O})$  vs elevation for MOD (black points) and INT (blue points) and isotopic gradients for the southern region (between 25°N and 30°N). Black line shows relationship from the empirical model (Rowley, 2001; Rowley and Garzzone, 2007). Green line shows second order polynomial approximation of simulated MOD  $\delta^{18}\text{O}$  values. Red line shows a linear regression for the INT  $\delta^{18}\text{O}$  values.

**R3 :** “ There is a bit of a cottage industry in the isotope-enabled GCM field looking at

1 *how isotope paleoaltimetry does/doesn't work in different orogenic systems. I would*  
2 *encourage the authors not to fall into the trap of saying "its complicated and you need to*  
3 *take additional factors into account." (This is essentially what is said at the end of the*  
4 *abstract.) Rather, make the information accessible and useful to the readers. Be specific*  
5 *and helpful in the abstract and throughout so that it is directly clear to the readers what*  
6 *specific factors are actually important and how they should be accounted for when*  
7 *reconstructing paleoaltimetry."*

8 **A:** We totally agree. Text will be corrected accordingly. We also provide estimates of  
9 contribution of different decomposition terms to the total isotopic signal for locations  
10 where previous paleoelevation studies have been done in the Table. 3.

11  
12 **Response to Specific Comments:**

13 **R3:** "P2 L16-18 – *Not all of these references are carbonates or oxygen isotopes*"

14 **A:** Thank you, these references has been replaced by: (Currie et al., 2005; DeCelles et al.,  
15 2007; Garzione et al., 2000; Rowley and Currie, 2006; Saylor et al., 2009; Xu et al.,  
16 2013; Li et al., 2015)

17  
18 **R3:** "P3 L4 – *most studies do take into account changing seawater  $\delta^{18}\text{O}$  either implicitly*  
19 *through normalization to a low elevation rainfall site or explicitly through correction*  
20 *using various estimates."*

21 **A:** Our purpose here was to show how climate changes have been thought to change the  
22  $\delta^{18}\text{O}$  record. We don't discuss here where these corrections used to be applied to  
23 paleoelevation reconstructions. We suggest to modify this sentence in this way:  
24 "Moreover, it has been suggested that climate-driven changes in surface ocean  $\delta^{18}\text{O}$   
25 through the Cenozoic can also influence recorded values of precipitation  $\delta^{18}\text{O}$  over the  
26 continent and an appropriate corrections has been applied in most modern studies."

27  
28 **R3:** "P3 L21 – *Seems that studies of Ramstein and Fluteau should be mentioned here."*

29 **A:** Thank you, we have added this reference.

30  
31 **R3:** "P7 L5 – *Is the assumption that sensitivity of the partial derivatives to state is not*  
32 *important ok? It seems this would be fairly easy to test by some simple calculations and*  
33 *then it could be definitively stated."*

1 **A:** We will address this point in the revised version of the manuscript.

2  
3 **R3:** *“P11 L1 – Are the Ddts values precipitation weighted? In general are the climatic*  
4 *variables used in the decomposition precipitation weighted? They should be.”*

5 **A:** Now we weight the decomposing terms by precipitation.

6  
7 **R3:** *“P11 L7-10 – How much of the temperature changes are due to comparison to a*  
8 *constant adiabat for all experiments? The adiabats that matter are only ones when*  
9 *moisture is being transported on to the plateau (non-linear with elevation) and the slope*  
10 *should change with T and q<sub>0</sub>. Thus, inference of non-adiabatic temperature changes*  
11 *could simply reflect the way this is calculated and not actual changes.”*

12 **A:** We thank reviewer for making a point on this. First of all we need to note that using  
13 of one mean lapse rate (in this paper equal to 5° km<sup>-1</sup> based on the measurements of  
14 modern observed mean temperature lapse rate on the southern slope of the central  
15 Himalayas) is clearly idealized. In our calculations we neglect the non-linearity of lapse  
16 rate. We agree that in addition to the effect of climate changes, the lapse rate is also  
17 affected by the humidity and temperature of the rising parcels. We will acknowledge this  
18 limitation in the revised version.

19  
20 **R3:** *“P12 L28-30 – One expects a non-linear relationship between rainfall isotope values*  
21 *and elevation simply because of the non-linearity of (i) saturated adiabats, (ii) the*  
22 *saturation vapor pressure curve with temperature and (iii) the Rayleigh distillation*  
23 *process itself. Thus the null hypothesis is that isotope changes with elevation from low to*  
24 *intermediate elevations would be less than isotope changes from intermediate to high*  
25 *elevations. Whether the changes are greater than can be explained by the null hypothesis*  
26 *needs to be demonstrated. But, the qualitative observation itself is actually expected from*  
27 *theory.”*

28 **A:** We agree. But interestingly, up to our knowledge, this null hypothesis that isotope  
29 changes with elevation from low to intermediate elevations would be less than isotope  
30 changes from intermediate to high elevations have never been discussed before in the  
31 paleoaltimetry literature. We agree with the reviewer that this conclusion is a logic  
32 consequence of non-linearity of saturated adiabats, the saturation vapour pressure curve  
33 with temperature and the Rayleigh distillation process. However we find useful to stress

1 this interesting characteristic for the geological community. The estimation whether the  
2 changes are greater than can be explained by the null hypothesis is out of scope of the  
3 paper and may be a subject of another study.

4  
5 **R3:** *“P14 L1 – Effects from post-condensation re-evaporation. This should have a  
6 distinct d-excess signal that should be evident in the model values. Examination of the d-  
7 excess signal spatially could directly answer this question.”*

8 **A:** Unfortunately we didn't include hydrogen isotopes in the simulations presented in this  
9 paper. Zoomed experiments including the isotopes are very expensive in terms of  
10 computation time (about 700 days of single CPU core time per experiment with only  
11 oxygen isotopes) and the calculation time increases linearly with every one additional  
12 isotope. However, with the numerical simulation we have an access to  $\delta^{18}\text{O}$  in both  
13 precipitation and vapour that gives a possibility to estimate the magnitude of post-  
14 condensation processes without appealing to the d-excess.

15  
16 **R3:** *“P15 L1 – How do these results compare with those of Boos and Kuang (2010)?”*

17 **A:** Although our purpose totally differs from B&K2010, our results in terms of monsoon  
18 dynamics seem very consistent. The no-elevation run from B&K2010 depicts a weaker  
19 monsoon and lower rainfall over Asia (Fig3b, Fig4A in their study).

20  
21 **R3:** *“P17 L15-16 – “Paleoelevation studies indicate the Himalayas attained their  
22 current elevation by the late Miocene.” This is not correct. Rowley and Currie (2006)  
23 and subsequent authors indicate earlier timing for modern elevations (middle Eocene or  
24 earlier).”*

25 **A:** Thank you for this correction. In fact, we show that for the southern part of the TP and  
26 Himalayas, paleoelevations based on stable oxygen isotopes measurement could be  
27 overestimated. We will modify our text accordingly.



# Impacts of Tibetan Plateau uplift on atmospheric dynamics and associated precipitation $\delta^{18}\text{O}$

S. Botsyun<sup>1</sup>, P. Sepulchre<sup>1</sup>, C. Risi<sup>2</sup>, and Y. Donnadieu<sup>1</sup>

[1]{Laboratoire des Sciences du Climat et de l'Environnement, LSCE/IPSL, CEA-CNRS-UVSQ, Université Paris-Saclay, Gif-sur-Yvette, France}

[2]{Laboratoire de Météorologie Dynamique, LMD/IPSL, UPMC, CNRS, Paris, France}

Correspondence to: S. Botsyun (svetlana.botsyun@lsce.ipsl.fr)

## Abstract

Paleoelevation reconstructions of mountain belts have become a focus of modern science since surface elevation provides crucial information for understanding both geodynamic mechanisms of Earth's interior and influence of mountains growth on climate. Stable oxygen isotopes paleoaltimetry is one of the most popular techniques nowadays, and relies on the difference between  $\delta^{18}\text{O}$  of paleo-precipitation reconstructed using the natural archives, and modern measured values for the point of interest. Our goal is to understand where and how complex climatic changes linked with the growth of mountains affect  $\delta^{18}\text{O}$  in precipitation. For this purpose, we develop a theoretical expression for the precipitation composition **based on the Rayleigh distillation and** the isotope-equipped atmospheric general circulation model LMDZ-iso **outputs**. Experiments with reduced height over the Tibetan Plateau and the Himalayas have been designed. Our results show that the isotopic composition of precipitation is very sensitive to climate changes related with the growth of the Himalayas and Tibetan Plateau. **Specifically our simulations suggest that only 40% of sampled sites for paleoaltimetry depict a full topographic signal, and that uplift-related changes in relative humidity (northern region) and precipitation amount (southern region) could explain absolute deviations of up to 2.5‰ of the isotopic signal, thereby creating biases in paleoelevation reconstructions.**

## 1    **1    Introduction**

2    Despite ongoing debates regarding the thermal and mechanical nature of  
3    mechanisms involved (Boos, 2015; Chen et al., 2014), the Himalayas and the Tibetan  
4    Plateau (hereafter TP) have long been considered to exert major influences on Asian  
5    atmospheric dynamics, notably by reinforcing South Asian monsoon and driving  
6    subsidence ultimately leading to onsets of deserts over Central Asia (Rodwell and  
7    Hoskins, 2001; Broccoli and Manabe, 1992). Thus, reconstructing the history of  
8    Himalayas and TP uplift appears crucial to understand long-term climate evolution  
9    of Asia. On the other hand, ~~topography uplift of TP is ultimately driven by collision~~  
10   ~~between India and Asia continents (Molnar et al., 2010), making~~ the timing and scale  
11   of surface elevation growth ~~are~~ widely used for reconstructing the rate and style of  
12   this tectonic plates convergence (eg. Royden et al., 2008; Tapponnier et al., 2001).

13   Elevation reconstructions for the Tibetan Plateau and Himalayas are based on fossil-  
14   leaf morphology (eg. Antal, 1993; Forest et al., 1999; Khan et al., 2014; (Sun et al.,  
15   2015), pollen (Dupont-Nivet et al., 2008), correlation between stomatal density and  
16   the decrease in CO<sub>2</sub> partial pressure with altitude (McElwain, 2004), and carbonate  
17   oxygen isotopic compositions (Currie et al., 2005; DeCelles et al., 2007; Garzione et  
18   al., 2000a; Li et al., 2015; Rowley and Currie, 2006; Saylor et al., 2009; Xu et al.,  
19   2013). In contrast to paleobotanical methods, oxygen isotope paleoaltimetry has  
20   been widely applied ~~to~~ the Cenozoic. Carbonate  $\delta^{18}\text{O}$  is related to topography change  
21   using  $\delta^{18}\text{O}$ -elevation relationship. These relationships have been calibrated both  
22   empirically (Garzione et al., 2000b; Gonfiantini et al., 2001; Poage and Chamberlain,  
23   2001) and theoretically, using basic thermodynamic principles, including Rayleigh  
24   distillation, that govern isotopic fractionation processes (Rowley and Garzione,  
25   2007; Rowley et al., 2001).

26   The difference between paleoprecipitation  $\delta^{18}\text{O}$  detected from natural archives and  
27   modern values of the site of interest is identified with the effect of the surface uplift  
28   in numerous recent studies (Currie et al., 2005; Cyr et al., 2005; Ding et al., 2014;  
29   Hoke et al., 2014; Mulch, 2016; Rowley and Currie, 2006; Rowley et al., 2001; Xu et  
30   al., 2013). In the absence of direct measurements of “paleo” altitude- $\delta^{18}\text{O}$   
31   relationship *in situ*, stable-isotope paleoaltimetry is potentially hampered by the fact  
32   that the presumed constancy of altitude- $\delta^{18}\text{O}$  relationships through time might not

1 be valid. For instance for the Andes, not considering the impact of uplift on climate  
2 dynamics and related  $\delta^{18}\text{O}$  values has been shown to produce errors in  
3 paleoelevation reconstruction reaching up to  $\pm 50\%$  (Ehlers and Poulsen, 2009;  
4 Poulsen et al., 2010). Regional climate variables and associated isotopic signal in  
5 precipitation can also be affected by global climate change (Battisti et al., 2014;  
6 Jeffery et al., 2012; Poulsen and Jeffery, 2011). Moreover, it has been suggested that  
7 climate-driven changes in surface ocean  $\delta^{18}\text{O}$  through the Cenozoic can also  
8 influence recorded values of precipitation  $\delta^{18}\text{O}$  over the continent and corrections  
9 has been applied in some studies (Ding et al., 2014). Over TP, mismatches between  
10 paleoelevation estimations from palynological and stable isotope data (eg. Sun et al.,  
11 2014) could be related to complex climatic changes and associated variations of  
12 altitude- $\delta^{18}\text{O}$  relationship linked to the uplift, but still a detailed assessment of the  
13 consequences of topographic changes on precipitation  $\delta^{18}\text{O}$  is lacking.

14 Spatial distribution of isotopes in precipitation was described using various types of  
15 models, from one-dimensional to three-dimensional general circulation (Craig,  
16 1961; Dansgaard, 1964; Gedzelman and Arnold, 1994; Risi et al., 2010; Stowhas and  
17 Moyano, 1993). Such modelling studies show how large-scale Asian monsoon  
18 circulation influence precipitation  $\delta^{18}\text{O}$  (He et al., 2015; LeGrande and Schmidt,  
19 2009; Pausata et al., 2011; Vuille et al., 2005). At the global scale, precipitation  $\delta^{18}\text{O}$   
20 has been shown to be affected by several factors other than elevation, including  
21 mixing between air masses (Ehlers and Poulsen, 2009; Gat, 1996), large-scale  
22 subsidence (e.g. Frankenberg et al., 2009), continental recycling (Lee et al., 2012;  
23 Risi et al., 2013), deep convection (Risi et al., 2008), and enrichments linked to  
24 global warming (Poulsen and Jeffery, 2011). Numerous studies have investigated  
25 the impact of Asian topography on climate change, including the monsoon  
26 intensification (ex. An et al., 2015; Harris, 2006a; Kutzbach et al., 1989; Ramstein et  
27 al., 1997; Raymo and Ruddiman, 1992; Zhang et al., 2015) and Asian interior  
28 aridification onset (Broccoli and Manabe, 1992; Liu et al., 2015). Nonetheless the  
29 linkage between these “climatic parameters” altered by the growth of TP and their  
30 influence on the isotopic signal remain unclear. In this article we use numerical  
31 modelling to provide some insights.

## 2 Methods

### 2.1 Model simulations

We use an Atmospheric General Circulation model (GCM) developed at Laboratoire de Météorologie Dynamique, Paris, France with isotopes-tracking implement, called LMDZ-iso (Risi et al., 2010). LMDZ-iso is derived from the LMDz model (Hourdin et al., 2006) that has been used for numerous future and paleoclimate studies (Ladant et al., 2014; Pohl et al., 2014; Sepulchre et al., 2006). Water in a condensed form and its vapour are advected by the Van Leer advection scheme (Van Leer, 1977). Isotopic processes in LMDZ-iso are documented in (Risi et al., 2010). Evaporation over land is assumed not to fractionate, given the simplicity of the model surface parameterisation (Risi et al., 2010). Yao et al. (2013) have provided a precise description of rainfall patterns over the TP, and showed LMDZ-iso ability to simulate atmospheric dynamics and reproduce rainfall and  $\delta^{18}\text{O}$  patterns consistent with data over this region.

LMDZ-iso is also equipped with water tagging capabilities, allowing us to quantify different moisture contributions from continental and oceanic evaporation sources. The advantage of this technique compared to typical back-trajectories methods is that it tracks the water rather than air masses, thus taking into account effects of phase changes. In our simulations five potential moisture sources are considered: (1) continental sources, (2) Indian Ocean, (3) Atlantic Ocean, (4) Mediterranean Sea, and (5) Pacific Ocean.

We use a model configuration with 96 grid points in longitude, 72 in latitude and 19 vertical layers, with the first four layers in the first kilometer above the surface. LMDZ-iso has a stretchable grid that allows increased spatial resolution over a defined region. In our case, it gives an averaged resolution of  $\sim 100$  km over central Asia, which is a good trade-off between a reasonable computing time and a spatial resolution that adequately represents main features of TP topography.

Here we report results from three experiments designed to isolate the influence of Asian topography on climate and isotopic composition of precipitation. Topography is derived from a 10-minute US Navy dataset and interpolated to the model grid. The control run (MOD) is a pre-industrial run, i.e. initialized with boundary conditions (insolation, greenhouse gases, sea surface temperatures (SSTs), topography) kept at

pre-industrial values. For the two other experiments, we keep all boundary conditions (including albedo, rugosity, and vegetation distribution) similar to those in MOD run, except for the topography. We reduce the altitude over the area covering the Tibetan Plateau, Himalayas and a part of surrounding mountains: Tian Shan, Pamir, Kunlun and Hindu Kush to 50% of modern elevations (intermediate, INT case) and to 250-m elevation (low, LOW case) (Fig. 1). SSTs for all runs come from the AMIP dataset (monthly SSTs averaged from 1979 to 1996; Taylor et al., 2000). Each experiment has been run for 20 years. We analyse seasonal means over the last 18 years, as the two first years are extracted for spin-up.

## 2.2 Theoretical framework for the precipitation composition

Our goal is to understand to what extent topography changes explain the precipitation  $\delta^{18}\text{O}$  signal over TP (i.e. the direct topography effect) and what part of this signal depends on other climate processes. To do so, we develop a theoretical expression for the precipitation composition.

To the first order, the  $\delta^{18}\text{O}$  composition of the precipitation  $R_p$  follows that of the vapour  $R_v$ . Deviations from the vapour composition,  $\varepsilon = R_p - R_v$ , are associated with local condensational or post condensational process.

$$R_p = R_v + \varepsilon \quad (1)$$

In an idealized framework of an isolated air parcel transported from an initial site at low altitude to the site of interest (Fig. 2), the vapour composition can be predicted by Rayleigh distillation:

$$R_v = R_{v0} \cdot f^{\alpha-1} + \delta R_v \quad (2)$$

where  $R_{v0}$  is the initial composition of the vapour at the initial site,  $\alpha$  is the fractionation coefficient, that depends on temperature and on the water phase (Majzoub, 1971; Merlivat and Nief, 1967), and  $f$  is the residual fraction of the vapour at the site of interest relatively to the initial site. We take the initial site as characterised by a temperature and humidity  $T_0$  and  $q_0$ . Under these conditions,  $R_{v0}$  is the theoretical isotopic composition of vapour that it would have if all the vapour originated from the local evaporation over quiescent oceanic conditions. Depending on the atmospheric circulation, on deep convective and mixing processes and on the source region of water vapour, the isotopic composition of vapour may deviates from the Rayleigh distillation by  $\delta R_v$ .

The residual fraction  $f$  depends on the specific humidity  $q$  at the site of interest:

$$f = q/q_0 \quad (3)$$

The air is not always saturated near the surface:

~~where  $q_s$  is the saturation specific humidity, function of temperature following the Clausius-Clapeyron relationship.~~

~~If we assume that the air at the site of interest has been transported adiabatically from the area of minimum condensation temperature, then:~~

$$q = h \cdot q_s(T_s) \quad (4)$$

where  $h$  and  $T_s$  are the relative humidity and air temperature near the surface of the site of interest. The air can be under-saturated because it can be considered as air that has been transported adiabatically from the area of minimum condensation temperature,  $T^*$  (Galewsky and Hurley, 2010; Galewsky et al., 2005; Sherwood, 1996):  $q = q_s(T^*)$

The surface temperature can be predicted to first order by the adiabatic lapse rate,  $\Gamma$ , and is modulated by the non-adiabatic component  $\delta T_s$  that represents processes such as large-scale circulation or radiation:

$$T_s = T_0 + \Gamma \cdot (z - z_0) + \delta T_s \quad (5)$$

where  $z$  and  $z_0$  are the altitudes at the site of interest and at the initial site. We use an adiabatic lapse rate equal to  $5^\circ \text{ km}^{-1}$  based on the measurements of modern observed mean temperature lapse rate on the southern slope of the central Himalayas, that ranges from  $4.7$  to  $6.1^\circ \text{ km}^{-1}$  for the monsoon season and from  $4.3$  to  $5.5^\circ \text{ km}^{-1}$  for the rest of the year (Kattel et al., 2015).

If we combine Eq. (1) to Eq. (5), we get that  $R_v$  is a function of  $\varepsilon$ ,  $\delta R_v$ ,  $h$ ,  $\delta T_s$  and  $z$ :

$$R_p = R_{v0} \cdot [h \cdot q_s(T_0 + \Gamma \cdot (z - z_0) + \delta T_s)/q_0]^{\alpha-1} + \delta R_v + \varepsilon \quad (6a)$$

Or in a simpler form:

$$R_p = R_p(\varepsilon, \delta R_v, h, \delta T_s, z) \quad (6b)$$

Parameters  $z_0$ ,  $q_0$ ,  $T_0$  are reference values that are common to all sites of interest, all climates and geographies. Even if initial conditions for the Rayleigh distillation vary depending on the atmosphere circulation, on deep convective processes and on the site of interest, we keep the same reference values and we consider all variations in initial conditions are accommodated by  $\delta R_v$ .

This model is equivalent to that of Rowley et al. (2001) for  $\delta R_v = 0$  (i.e. neglecting the effects of mixing and deep convection on the initial water vapour),  $\varepsilon = (\alpha - 1) \cdot R_v$  (i.e. neglecting post-condensational effects), and  $h = 1$  (i.e. assuming the site of interest is inside the precipitating cloud).

### 2.3 Decomposing precipitation composition differences

Our goal is to understand why  $R_p$  varies from one climatic state to another. We refer to these climatic states using subscript 1 and 2 and to their difference using the  $\Delta$  notation. Differences between INT and LOW and between MOD and INT climatic states corresponds to the initial and the terminate stages of the TP uplift respectively. We decompose  $\Delta R_p = R_{p2} - R_{p1}$  into contribution from  $\Delta \delta R_v$ ,  $\Delta \varepsilon$ ,  $\Delta h$ ,  $\Delta \delta T_s$ , and  $\Delta z$ :

$$\Delta R_p = \frac{\partial R_p}{\partial \delta R_v} \cdot \Delta \delta R_v + \frac{\partial R_p}{\partial \varepsilon} \cdot \Delta \varepsilon + \frac{\partial R_p}{\partial h} \cdot \Delta h + \frac{\partial R_p}{\partial \delta T_s} \cdot \Delta \delta T_s + \frac{\partial R_p}{\partial z} \cdot \Delta z \quad (8)$$

$$\Delta R_p = \Delta R_{p,\Delta \varepsilon} + \Delta R_{p,\Delta \delta R_v} + \Delta R_{p,\Delta h} + \Delta R_{p,\Delta \delta T_s} + \Delta R_{p,\Delta z} + N \quad (7)$$

Where  $\Delta R_{p,\Delta \varepsilon}$ ,  $\Delta R_{p,\Delta \delta R_v}$ ,  $\Delta R_{p,\Delta h}$ ,  $\Delta R_{p,\Delta \delta T_s}$ , and  $\Delta R_{p,\Delta z}$  are respectively the contributions of  $\Delta \delta R_v$ ,  $\Delta \varepsilon$ ,  $\Delta h$ ,  $\Delta \delta T_s$ , and  $\Delta z$  to  $\Delta R_p$ . Non linear terms of decomposition are gathered into the residual term  $N$ . Contributions are estimated using equation 6 (see also Table 1):

$$R_{p,\Delta \varepsilon} = R_p(\varepsilon_2, \delta R_v', h', \delta T_s', z') - R_p(\varepsilon_1, \delta R_v', h', \delta T_s', z') \quad (8)$$

$$R_{p,\Delta \delta R_v} = R_p(\varepsilon', \delta R_{v2}, h', \delta T_s', z') - R_p(\varepsilon', \delta R_{v1}, h', \delta T_s', z') \quad (9)$$

$$R_{p,\Delta h} = R_p(\varepsilon', \delta R_v', h_2, \delta T_s', z') - R_p(\varepsilon', \delta R_v', h_1, \delta T_s', z') \quad (10)$$

$$R_{p,\Delta \delta T_s} = R_p(\varepsilon', \delta R_v', h', \delta T_{s2}, z') - R_p(\varepsilon', \delta R_v', h', \delta T_{s1}, z') \quad (11)$$

$$R_{p,\Delta z} = R_p(\varepsilon', \delta R_v', h', \delta T_s', z_2) - R_p(\varepsilon', \delta R_v', h', \delta T_s', z_1) \quad (12)$$

In order to decrease the sensitivity of the decomposition to the state at which it has been calculated we take  $z'$ ,  $\delta T_s'$ ,  $h'$ ,  $\delta R_v'$ , and  $\varepsilon'$  as centred differences:

$$z' = (z_2 + z_1)/2 \quad (13)$$

$$\delta T_s' = (\delta T_{s2} + \delta T_{s1})/2 \quad (14)$$

$$h' = (h_2 + h_1)/2 \quad (15)$$

$$\delta R_v' = (\delta R_{v2} + \delta R_{v1})/2 \quad (16)$$

$$\varepsilon' = (\varepsilon_2 + \varepsilon_1)/2 \quad (17)$$

Note that  $\varepsilon'$  in Equations 9 to 12 and  $\delta R_v'$  in Equations 8 and 10 to 12 can be replaced by 0 without changing the result. Parameters  $z$ ,  $\delta T_s$ ,  $h$ ,  $\delta R_v$ , and  $\varepsilon$  are diagnosed for the climatic states 1 and 2 from LMDZ-iso simulations (ex. for pairs of

experiments, MOD and INT cases). Parameter  $\varepsilon$  is estimated as  $\varepsilon = R_p - R_v$ , where  $R_p$  and  $R_v$  are isotopic ratios simulated by LMDZ-iso. Parameter  $h$  is the relative humidity simulated by LMDZ-iso. Altitude  $z$  is a prescribed boundary condition of the simulations. Parameter  $\delta R_v$  is estimated by calculating the difference between the water vapour isotopic ratio simulated by LMDZ-iso ( $R_{v,LMDZ}$ ) and that predicted by Rayleigh distillation if the initial water vapour isotopic ratio is  $R_{v0}$ :

$$\delta R_v = R_{v,LMDZ} - R_{v0} \cdot (q/q_0)^{\alpha-1} \quad (18)$$

where  $q$  is the specific humidity simulated by LMDZ-iso and  $\alpha$  is the isotopic fractionation as a function of the near-surface air temperature  $T_s$  simulated by LMDZ-iso. Parameter  $\delta T_s$  is estimated from equation (5) by calculating the difference between the near-surface air temperature simulated by LMDZ-iso and that predicted by the adiabatic lapse rate:

$$\delta T_s = T_s - T_0 - \Gamma \cdot (z - z_0) \quad (19)$$

~~To estimate each of these terms, we estimate difference between  $R_p$  calculated from the different values of  $\delta R_{vi}$ ,  $\varepsilon$ ,  $h$ ,  $\delta T_s$ , and  $z$ , changing only one parameter at a time, as detailed in table 1 (and see next section).~~

~~Values of  $\delta R_{vi}$ ,  $\varepsilon$ ,  $h$ ,  $\delta T_s$ , and  $z$ , are diagnosed using LMDZ-iso simulations. As an example  $R_p(\delta R_{vi2}, \varepsilon_2, h_2, \delta T_{s2}, z_2)$  is the precipitation composition simulated by LMDZ for climate state 2. As another example,  $R_p(0, 0, 1, \delta T_{s1}, z_1)$  is the precipitation composition predicted by Eqs. (2)–(5) with  $\delta R_{vi} = 0$  and using the near-surface air temperature as  $T_s$  simulated by LMDZ for climatic state 1 (see Table 1).~~

All the isotopic decomposition terms computed are weighted by the precipitation amount.

## 2.4 Robustness of the decomposition

First, to check whether the linear decomposition is a good approximation of the total  $R_p$  change, we estimate the non-linear term  $N$  as a residual, i.e. for each pair of states, we calculate the deviation of  $\Delta R_p = R_p(\varepsilon_2, \delta R_{v2}, h_2, \delta T_{s2}, z_2) - R_p(\varepsilon_1, \delta R_{v1}, h_1, \delta T_{s1}, z_1)$  from LMDZ-simulated isotopic differences between the two experiments.  $N$  represents less than 17% of the total  $R_p$  change for both stages of TP uplift.

Our method to estimate the terms in Eq. (7) is equivalent to first order approximation of partial derivatives, i.e. we neglect the sensitivity of the partial derivatives to the state at which they are calculated. We tested this sensitivity by



using Eq. (8) to Eq. (12) changing  $z'$  to  $z_1$  or  $z_2$   $\delta T_s'$  to  $\delta T_{s2}$  or  $\delta T_{s1}$  and so on. For example, in Eq. (12), replacing of  $h'$  by  $h_1$  changes the resulting  $R_{p,\Delta z}$  by 0.03‰, replacing of  $h'$  by  $h_2$  has an impact of 0.09‰. In the same equation, replacing of  $\delta T_s'$  by  $\delta T_{s1}$  and by  $\delta T_{s2}$  contributes to  $R_{p,\Delta z}$  by 0.005‰ and 0.039‰ respectively. As it was highlighted earlier, replacing of  $\varepsilon'$  and  $\delta T_s'$  by  $\varepsilon_1$  or  $\varepsilon_2$  and  $\delta R_{v1}$  or  $\delta R_{v2}$  respectively has no impact to the resulting  $R_{p,\Delta z}$ . Thus our method show low sensitivity to the state.

Second, to check the influence of initial conditions  $R_{v0}$ ,  $T_0$  and  $q_0$  on the decomposition, we estimate the sensitivity of the different contributions to changes in  $R_{v0}$ ,  $T_0$ , and  $q_0$ , of 1‰, 1K and 10% respectively (Table 2).  $R_{v0}$  is the parameter that influences the most the decomposition terms, with a maximal sensitivity obtained of 0.9‰ for  $\Delta R_{p,\Delta z}$  for a change of 1‰ in  $R_{v0}$ . Sensitivity to temperature and humidity are lower, ranging from 0 to 0.6‰. Overall, all the decomposition terms show a sensitivity <1‰ with most (82%) of them <0.5‰, making our decomposition method robust.

### 3 Results

#### 3.1 Model validation in terms of simulated climate variables

LMDZ has been used for numerous present-day climate and paleoclimate studies (Kageyama et al., 2005; Ladant et al., 2014; Sepulchre et al., 2006), including studies of monsoon region (eg. Lee et al., 2012; Licht et al., 2014). Yao et al., (2013) showed that LMDZ-iso has the best representation of the altitudinal effect compared to similar GCM and RCM models. These authors also have provided a detailed description of rainfall patterns over the Tibetan Plateau, and showed LMDZ-iso ability to simulate atmospheric dynamics and reproduce rainfall and  $\delta^{18}\text{O}$  patterns consistent with data over this region. For the purpose of our experiments validation, we compare MOD experiment outputs with rainfall data from the Climate Research Unit (CRU) (New et al., 2002) (Fig. 3 A B C). When compared to CRU dataset, MOD annual rainfalls depict an overestimation over the high topography of the Himalayas and the southern edge of the Plateau, with a rainy season that starts too early and ends too late in the year. Over central Tibet (30-35°N), the seasonal cycle is well

captured by LMDz-iso, although monthly rainfall is always slightly overestimated (+0.5 mm/day). CRU data shows that the northern TP (35-40°N) is dryer with no marked rainfall season and a mean rainfall rate of 0.5 mm/day. In MOD experiment, this rate is overestimated (1.5 mm/day on annual average). Despite these model-data mismatches, the ability of LMDZ-iso to represent the seasonal cycle in the south and the rainfall latitudinal gradient over the TP allows its use for the purpose of this study.

Our MOD simulation is pre-industrial, consequently a comparison with modern data is expected to provide differences driven by the pre-industrial boundary conditions. Still comparing LMDZ-iso outputs with mean annual temperatures from CRU dataset (New et al., 2002) (Fig. 3 D E F) and relative humidity from NCEP-DOE Reanalysis (Kanamitsu et al., 2002) (Fig. S1) shows that LMDZ-iso model captures these variables reasonably well.

### 3.2 Impact of TP uplift on Asian climate

Theoretically, the Tibetan Plateau has both mechanical and thermal effects on atmospheric dynamics that induce increase monsoon activity to the south and drive arid climate to the north (Broccoli and Manabe, 1992; Sato and Kimura, 2005). Thus modifying TP height is expected to alter these large-scale atmospheric dynamics and associated climate variables (namely temperature, precipitation, relative humidity (hereafter RH), cloud cover), and in turn to affect the isotopic signature of rainfall.

In LOW experiment, strong summer heating leads to the onset of a “Thermal Low” (~~TL~~) at the latitude of maximal insolation (ca. 32°N), similar to the present-day structure ~~TL~~ existing over the Sahara desert (Fig. S2). This structure is superimposed by large-scale subsidence linked to the descending branch of the Hadley cell, and both factors act to drive widespread aridity over TP area between ca. 30°N and 40°N, associated with very low (<40%) RH values (Fig. S2). Subsidence also prevents the development of South Asian monsoon over the north Indian plane and favours aridity over this region. In winter, large-scale subsidence induces high surface pressures and creates an anticyclonic cell that prevents convection and humidity advection, resulting in low RH and annual rainfall amount ranging from 50 to 500 mm over TP area (Fig. 4).

Uplifting TP from 250m above sea-level (ASL) to half of its present-day altitude (INT case) initiates convection in the first tropospheric layers, **restricting** large-scale subsidence to the upper levels (Fig. 4). In turn, south Asian monsoon is strengthened and associated northward moisture transport and precipitation increase south of TP (Fig. 5, 6). As a consequence the hydrological cycle over TP is more active, with higher evaporation rates (Fig. 7 D). Together with colder temperatures linked to higher altitude (adiabatic effect) (Fig. 7 B), the stronger hydrological cycle drives an increase in RH (Fig. 7 A) and cloud cover (Fig. S3). Another consequence of increased altitude is higher snowfall rates in winter and associated rise of surface albedo (fig. S4). When added to the increased cloud cover effect, this last process contributes to an extra cooling of air masses over the Plateau. To the north of TP, the initial stage of uplift results in increased aridity (i.e. lower RH and rainfall) over the Tarim Basin region. This pattern can be explained both by a barrier effect of southern topography and by stationary waves strengthening, that results in subsidence to the north of TP. This latter mechanism is consistent with pioneer studies which showed that mountain-related activation of stationary waves prevented cyclonic activity over Central Asia and induced aridity over this region (Broccoli and Manabe, 1992).

The impact of the terminal stage of TP uplift also drives an increase in RH over the Plateau, especially during summer time, when a very active continental recycling (Fig. S6) makes RH rise from 40% (INT) to 70% (MOD). Precipitation amount also increases significantly (Fig. 6), driven both by increased evaporation and water recycling during summer, and intense snowfall during winter. The latter contributes to increase the surface albedo and associated surface cooling during winter. Conversely, the uplift to a modern-like Plateau reduces RH (down to 30%) north of the Plateau, and allows the onset of large arid areas. We infer that this aridification is linked to a mechanical blocking of moisture transport, both by Tian Shan topography for the winter westerlies, and the eastern flanks of TP for summer fluxes, since despite changes in stationary waves structure and sensible heat (not shown), no marked shift in subsidence between INT and MOD experiments is simulated. This result is consistent with recent studies (Miao et al., 2012; Sun et al., 2009) that have suggested the potential contribution of Pamir and Tian Shan

rainshadow effect to aridification in Qaidam Bassin and creation of Taklamakan Desert.

### 3.3 Response of precipitation $\delta^{18}\text{O}$ to TP uplift

#### 3.3.1 Model validation in terms of simulated precipitation $\delta^{18}\text{O}$

The modern mean annual isotopic distribution is characterised by very depleted values of  $\delta^{18}\text{O}$  over the Himalayas and the southern Tibet (down to  $-18\text{‰}$ ) and a shift to more positive values (ranges from  $-11$  to  $-13\text{‰}$ ) over northern TP and Kunlun from  $30^\circ\text{N}$  to  $35^\circ\text{N}$ . Precipitation  $\delta^{18}\text{O}$  over Tarim Basin experiences an abrupt decrease compared to northern TP, with values down to  $-16\text{‰}$ . (Fig. 8 A). Overall, simulated annual mean  $\delta^{18}\text{O}_p$  are consistent with sparse observations from the International Atomic Energy Agency (IAEA) Global Network of Isotopes in Precipitation and  $\delta^{18}\text{O}$  in precipitation measurements compiled from Quade et al. (2011), Bershaw et al. (2012), Hren et al. (2009), Caves et al. (2015) (Fig. 8 A B). In general, model shows a good agreement with precipitation and VSMOW-weighted modern surface waters  $\delta^{18}\text{O}$ , including stream, lake and spring waters (data from Bershaw et al., 2012; Hren et al., 2009; Quade et al., 2011), as testified by a Pearson coefficient of 0.86 between modelled and observed precipitation  $\delta^{18}\text{O}$  (Fig 8C). This comparison shows the ability of LMDZiso to reproduce the decrease in  $\delta^{18}\text{O}$  from India subcontinent to Himalayas foothills and with minimum values over the Himalayas. Simulated increase in  $\delta^{18}\text{O}$  over the TP with the distance from the Himalayas is also consistent with data sampled along a southwest-northeast transect across the Plateau (Bershaw et al., 2012). However over the northern margins of the TP, LMDZ-iso underestimates simulated  $\delta^{18}\text{O}$  in precipitation. This model-data mismatch may result from two types of uncertainties. First despite the high resolution obtained with a zoomed grid, restricted topographic features could be not well-captured over some parts of the TP, which could lead our simulations to miss local processes affecting  $\delta^{18}\text{O}$  in rainfall. Second, overestimating the westerlies fluxes (see the comparison with the ERA moisture transport on Fig. 5 A) could lead to underestimate  $\delta^{18}\text{O}$  over the northern part of the TP, through advection of depleted air masses. Nevertheless, despite our model does not capture well the absolute maximal values, the regional latitudinal gradient is correctly represented,

1 and most observed values are within the range of simulated  $\delta^{18}\text{O}$  (Fig. 8B). We  
2 consider that the ability of LMDZ-iso to represent this gradient makes it reliable to  
3 carry out this study, which is focusing on sensitivity experiments with large changes  
4 in topography and associated anomalies in  $\delta^{18}\text{O}$ .

### 6 3.3.2 Simulated isotopic changes and signal decomposition

7 To first order, increasing topography over TP leads to more negative  $\delta^{18}\text{O}$  over the  
8 region (Fig. 9). In the absence of topography, precipitation  $\delta^{18}\text{O}$  follows a zonal  
9 pattern and undergoes a weak latitudinal depletion on the way to the continental  
10 interior, except from slight deviations over India ~~n-plane~~, central China and the  
11 Eastern part of the TP (Fig. 9 B). At 40°N, i.e. the northern edge of modern TP,  $\delta^{18}\text{O}$   
12 values reaches -9‰ in LOW case, compared to -14‰ in MOD case. For the INT case  
13 the latitudinal depletion from south to north is stronger (ca. 0.4‰ per latitudinal  
14 degree), with  $\delta^{18}\text{O}$  values ranging from -6‰ for the lowered Himalayas foothills to -  
15 11‰ for northern and eastern margins of TP (Fig. 9 A).

16 The total difference in isotopic composition of precipitation,  $\Delta R_p$ , between pairs of  
17 experiments (INT-LOW, MOD-INT) is significant beyond the areas where the  
18 topography was reduced by the experimental design (Fig. 10 A, Fig. 11 A).  
19 Substantial differences in  $\delta^{18}\text{O}$  between MOD and INT experiments are simulated  
20 over the southern TP (up to 10‰) and over the Tarim Basin (up to 7‰). Between  
21 INT and LOW cases, the differences are over the margins of the TP, over Pamir, Tian  
22 Shan and Nan Chan. We should note that the isotopic difference becomes more  
23 important for the later stage of the plateau uplift. For clarity, we define two boxes,  
24 over the northern (from 34°N to 38°N and from 88°E to 100°E) and southern (from  
25 27°N to 33°N and from 75°E to 95°E) part of TP.

### 27 Direct topography effect on $\delta^{18}\text{O}$

28 The direct effect of topography change is determined as the decomposition term  
29  $\Delta R_{p,\Delta z} \frac{\partial R_p}{\partial z} \cdot \Delta z$  in Eq. (7). For the initial stage of the uplift, the altitude effect produces  
30 a decrease in precipitation  $\delta^{18}\text{O}$  ranging from -1 to -3‰ (Fig. 10 B). For the terminal  
31 stage of the uplift, the isotopic decrease linked with altitude goes up to -7‰ (Fig. 11

B). Differences between both stages are linked to the non-linear relationship between  $\delta^{18}\text{O}$  and elevation. Also for both stages, the difference between  $\Delta R_p$  and  $\Delta R_{p,\Delta z} \frac{\partial R_p}{\partial z} \cdot \Delta z$  is non-zero (Fig. 12 A, Fig. 13 A). These differences are particularly marked for the terminal stage, for which  $\Delta R_{p,\Delta z} \frac{\partial R_p}{\partial z} \cdot \Delta z$  averages -5.5‰ over the northern part of TP (Fig. 13 A B), whereas the total isotopic change averages -3‰. Locally, the difference between  $\Delta R_{p,\Delta z} \frac{\partial R_p}{\partial z} \cdot \Delta z$  and  $\Delta R_p$  can reach +4‰. When averaged over the southern box,  $\Delta R_{p,\Delta z} \frac{\partial R_p}{\partial z} \cdot \Delta z$  is less negative (-4‰) than  $\Delta R_p$  (-4.6‰), with localized maximum differences reaching -4‰. Offsets between  $\Delta R_{p,\Delta z} \frac{\partial R_p}{\partial z} \cdot \Delta z$  and  $\Delta R_p$  are also detected for the initial stage of the uplift (Fig. 12 A B), but are lower: they reach +2‰ over central TP but barely reach 1‰ when averaged over southern and northern boxes. These offsets are related to additional effects of uplift on  $\delta^{18}\text{O}$  that are discussed in the following sections.

#### Non-adiabatic temperature changes impact

Besides the adiabatic temperature effects linked with the TP uplift, non-adiabatic temperature changes can be identified, in relation with surface albedo and cloud cover changes depicted in 3.2.1. The term  $\Delta R_{p,\Delta \delta T} \frac{\partial R_p}{\partial \delta T_s} \cdot \Delta \delta T_s$  in Eq. (7) (Table 1, line 3) is associated with these non-adiabatic effects, i.e. spatial variations of the temperature lapse rate. Figure 10 C and Figure 11 C show the portion of the total isotopic signal that is linked to this effect. It plays a modest role for the early phase of uplift (+1-2‰ locally), but is more important for the second stage. It contributes to 2-5‰ of total isotopic difference, with a positive sign over southeast TP interior, TP northern margins and Asia interior. Negative anomalies have the same a magnitude of 2-3‰, but are less widespread, localized over the TP interior (Fig. 11 C). Positive isotopic anomalies are associated with steeper lapse rate than expected based on adiabatic processes. Conversely, negative  $\delta^{18}\text{O}$  anomalies that are observed over northern TP and over Pamir are explained by a weaker lapse rate than adiabatic. Overall, these variations represent between 10 and 19% (4-10% for the initial stage) of the processes that are not linked to topography (Fig. 12 D, E and 13 D, E).

## Impact of RH changes during condensation process

The term  $\Delta R_{p,\Delta h} \frac{\partial R_p}{\partial h} \cdot \Delta h$  in Eq. (7) depicts the portion of total isotopic signal  $\Delta R_p$  linked to local RH change during condensation process (Table. 1, line 4). Over TP,  $\Delta R_{p,\Delta h} \frac{\partial R_p}{\partial h} \cdot \Delta h$  is positive for both uplift phases, and RH changes act as a counterbalance to the topography effect.  $\Delta R_{p,\Delta h} \frac{\partial R_p}{\partial h} \cdot \Delta h$  reaches +4‰ for the late stage (Fig. 11 D), and maxima are located over western part and northern part of TP for both stages of the uplift. Equation (4) shows that this positive anomaly is directly related to the increase in RH described in 3.2.1. For the initial stage,  $\Delta R_{p,\Delta h} \frac{\partial R_p}{\partial h} \cdot \Delta h$  depicts also positive values (up to +3‰) to the southwest of TP. When averaged over northern and southern boxes, the counterbalancing effect of RH on  $\Delta R_p$  ranges from 1.5 to +3‰, and this effect represents up to 76% of all non-topographic processes (Fig. 12, 13). Interestingly, an opposite signal is simulated over the Tarim basin, where topography was kept constant in the three experiments. This signal is consistent with the previously-depicted decrease in RH over this region, in relation with rain-shadow effects and large-scale subsidence.

## Post-condensation processes impact

The difference between  $\delta^{18}\text{O}_v$  and  $\delta^{18}\text{O}_p$  is linked to the post-condensation effects, mainly associated with raindrop reevaporation that can occur after initial condensation. Because lighter isotopes evaporate more easily, rain reevaporation leads to an isotopic enrichment of precipitation. Therefore, the more reevaporation, the greater the difference between  $\delta^{18}\text{O}_p$  and  $\delta^{18}\text{O}_v$ . We refer to the study of (Lee and Fung, 2008), where post-condensation effects are explained in details. The contribution of such processes increases dramatically for very dry areas, where the relative humidity is less than 40%. Estimation of term  $\Delta R_{p,\Delta \epsilon} \frac{\partial R_p}{\partial \epsilon} \cdot \Delta \epsilon$ , i.e. the change in isotopic difference between vapour and precipitation, allows to quantify the contribution of post-condensational processes to total  $\Delta R_p$  signal (Fig. 10 E, 11 E) without appealing to the d-excess. For both stages of uplift,  $\Delta R_{p,\Delta \epsilon} \frac{\partial R_p}{\partial \epsilon} \cdot \Delta \epsilon$  is mostly negative, indicating a depletion of  $R_p$  relatively to  $R_v$  with the uplift. Over the Plateau,



contribution of post-condensational effects for the initial stage of uplift ranges from 25% to 46% of total non-topographic effects, whereas it represents less than 10% for the terminal stage (Fig. 12 A, 13 A). The most significant signal is simulated over the northern part of the Plateau and over its western margin and adjacent areas. Post-condensational effects during the initial stage lead to up to a -5‰ anomaly over the western margin of TP (Fig. 12 E) whereas the terminal stage creates a substantial negative anomaly only over northern TP margin and Tarim Basin (Fig. 13 E).

## Residual processes effect

The last term of Eq. (7),  $\Delta R_{p,\Delta\delta R_v} \frac{\partial R_p}{\partial R_{pt}} \cdot \Delta\delta R_{pt}$ , corresponds to the part of the total isotopic signal that could not be explained by previously mentioned processes. These residual anomalies are rather weak for the initial stage of the uplift, explaining less than 1‰ of the signal over the northern plateau, and around 1‰ over the southern TP and adjacent parts of Asia and India (Fig. 10 F). Contribution of these effects to the initial stage is 4% and 21% to the northern and southern box respectively (Fig. 12 D E). Conversely, for the terminal stage of the TP uplift this anomaly reaches up to -4‰ over the southern part of the TP (Fig. 11 F) and contributes to 49% of the non-topographic processes signal (Fig. 13 D E). In the next sections we propose several mechanisms that could contribute to this residual anomaly.

## 4 Discussion

Our results suggest that TP uplift affects precipitation  $\delta^{18}\text{O}$  through direct topographic effect, but that a significant part of the signal is related to several other processes. These processes alter the isotopic signal not only over TP, but also over adjacent regions, where topography was kept the same by the experiment design. A second result is that despite a similar altitudinal change of TP between the two uplift stages, the topographic effect on  $\delta^{18}\text{O}$  is more perturbed by other processes during the terminal stage than during the initial one.

For the terminal stage, the residual effects change over the southern region dominates (49%) the isotopic signal that is not linked to the direct topographic



effect. The RH change and non-adiabatic temperature changes also have an important counterbalancing impact, together contributing to 43% of the isotopic signal (Fig. 13 E). For the northern region, the topographic effect is mainly counterbalanced by the RH change effect (2.5‰), ultimately leading to a 2.3‰ offset between  $\Delta R_p$  and what expected from topography. Here RH contributes to 76% of the isotopic signal not linked with the topography change, while non-adiabatic temperature changes, residual effects change and post-condensational processes have an impact of 16%, 7% and <1% respectively (Fig. 13 D).

#### 4.1 Impact of RH variations

RH alters rainfall isotopic signature through two steps, during and after condensation. As mentioned earlier, the first effect of RH, as shown in Eq. (4) and expressed as  $\Delta R_{p,\Delta h} \frac{\partial R_p}{\partial h} \cdot \Delta h$ , occurs during condensation through Rayleigh distillation and induces that  $R_p$  increases with increasing RH. Our model shows that RH increases over TP with the initial stage of uplift, driving precipitation  $\delta^{18}\text{O}$  towards less negative values. This mechanism is more efficient for the terminal stage of uplift, when RH is increased in summer as a response of a more active water cycle. South of TP, RH direct effect on  $\delta^{18}\text{O}$  is noticeable, as efficient moisture transport is activated with the uplift-driven strengthening of monsoon circulation (Fig. 4). Interestingly, this mechanism is not active for the second stage of the uplift, during which rainfall increases through more effective convection, not through higher advection of moisture. As a consequence, negligible RH and  $R_p$  changes are simulated south of the Plateau when it reaches its full height. This suggests that an altitudinal threshold might trigger south Asian monsoon strengthening, and ultimately precipitation  $\delta^{18}\text{O}$  signature, a hypothesis that should be explored in further studies. Conversely, the negative values of  $\Delta R_{p,\Delta h} \frac{\partial R_p}{\partial h} \cdot \Delta h$  over and northeast of the Tarim basin are related to a decrease in RH during both stages. Our analysis suggests that the first uplift stage is sufficient to create both barrier effects to moisture fluxes and large-scale subsidence that ultimately drive aridity over the region.

The second effect of RH on  $\delta^{18}\text{O}$  concerns very dry areas (ca. < 40%), where raindrop re-evaporation can occur after initial condensation, leading to an isotopic enrichment of precipitation compared to water vapour (Lee and Fung, 2008) (Fig. S2). Such an effect is implicitly included in the post-condensational term of our decomposition that shows opposite sign when compared to  $\Delta R_{p,\Delta h} \frac{\partial R_p}{\partial h} \cdot \Delta h$ . Over the Plateau, this mechanism is effective only for the first uplift stage, where TP area transits from very low precipitation amounts and very low RH values to wetter conditions (Fig. S7). Over TP, the opposed effects of RH almost compensate each other for the early stage of the uplift (Fig. 10 D, E), but it is not the case for the final stage, since RH post-condensational effect is similar between INT and MOD experiments. Since absolute values of the impact of RH through condensation and post-condensational processes can reach 5‰, it is crucial to consider RH variation when inferring paleoaltitudes from carbonates  $\delta^{18}\text{O}$ .

## 4.2 “Amount effect” and monsoon intensification

Our results also show a substantial increase in precipitation amount over northern India, the Himalayas and TP with the growth of topography for both uplift stages (Fig. 13). The inverse relation between the enrichment in heavy isotopes in precipitation and precipitation amount, named the “amount effect” (Dansgaard, 1964) is largely known for oceanic tropical conditions (Risi et al., 2008; Rozanski, Kazimierz Araguás-Araguás and Gonfiantini, 1993) and for Asia monsoonal areas (Lee et al., 2012; Yang et al., 2011). Over South Tibet recent studies have shown the role of deep convection in isotopic depletion (He et al., 2015). For the two stages of uplift, the residual component of the isotopic signal depicts negative values over southern TP, where annual rainfall amount is increased. Thus we infer that this anomaly can be driven, at least partly, by the amount effect that increases with growing topography.

Various climate studies have suggested that the appearance of the monsoonal system in East Asia and the onset of central Asian desertification were related to Cenozoic Himalayan–Tibetan uplift and withdrawal of the Paratethys Sea (An et al., 2001; Clift et al., 2008; Guo et al., 2002, 2008; Kutzbach et al., 1989, 1993; Ramstein

et al., 1997; Raymo and Ruddiman, 1992; Ruddiman and Kutzbach, 1989; Sun and Wang, 2005; Zhang et al., 2007) although the exact timing of the monsoon onset and its intensification remains debated (Licht et al., 2014; Molnar et al., 2010). Although our experimental setup, which does not include Cenozoic paleogeography, was not designed to assess the question of monsoon driving mechanisms nor its timing, our results suggest that uplifting the Plateau from 250 meters ASL to half of its present height is enough to enhance moisture transport towards northern India and strengthen seasonal rainfall. Nevertheless, massive increase of rainfall over TP between INT and MOD experiments indicates that the second phase of uplift might be crucial to activate an efficient, modern-day-like, hydrological cycle over the Plateau. The decrease in simulated precipitation north of the Plateau also suggests that terminal phase of TP uplift triggered modern-day arid areas.

### **4.3 Other effects**

Although precipitation amount change explains well the residual isotopic anomaly (Fig. 10 F, Fig. 11 F), additional processes could interplay. Continental recycling can overprint original moisture signature and shifts the isotopic ratios to higher values due to recharging of moisture by heavy isotopes from soil evaporation (Lee et al., 2012; Risi et al., 2013). In our simulation, we detect an increasing role of continental recycling in the hydrological budget of the TP (Fig. S6), especially in its central part, that likely shifts the  $\delta^{18}\text{O}$  to more positive values and partially compensate for the depletion linked to the “amount effect” over the central plateau. Another process frequently invoked to explain the evolution of precipitation  $\delta^{18}\text{O}$  patterns over TP is changes in moisture sources (Bershaw et al., 2012; Dettman et al., 2003; Quade et al., 2007; Tian et al., 2007). Except for the continentally recycled moisture, southern Himalayas precipitation moisture originates mainly from the Indian, the Atlantic and the Pacific Oceans (Fig. S6). Proximate oceanic basins are known to be sources of moisture with more positive signature than remote ones (Chen et al., 2012; Gat, 1996). Supplemental analyses with water-tagging feature of LMDZ-iso show that contribution of continental recycling to rainfall over TP increases with the uplift, at the expense of Pacific and Indian sources (Fig. S6). Although we have no mean to

decipher between sources and amount effect in the residual anomaly, it seems that the change of sources is not sufficient to yield a strong offset of  $\delta^{18}\text{O}$  values.

#### **4.4 Relevance of paleoelevation reconstructions based on paleo $\delta^{18}\text{O}$**

Quantitative paleoelevation reconstructions using modern altitude- $\delta^{18}\text{O}$  relationship will succeed only if  $\Delta R_p$  corresponds mainly to the direct topography effect. Modern paleoaltimetry studies cover almost all regions of the Plateau for time periods ranging from Palaeocene to Pleistocene-Quaternary (see data compilation in Caves et al., 2015). Most of these studies consider changes in  $\delta^{18}\text{O}$  as a direct effect of the topography uplift. Paleoelevation studies locations (see Caves et al., 2015 for a synthesis) plotted over the anomaly maps (Fig. 12 A, Fig. 13 A) show for what geographical regions restored elevations should be used with an additional caution. Numerous paleoelevation data points were located either over the northern part of the TP (from 34°N to 38°N and from 88°E to 100°E) or over the southern region (from 27°N to 33°N and from 75°E to 95°E).

Our model results show that when TP altitude is increased from half to full, considering topography as an exclusive controlling factor of precipitation  $\delta^{18}\text{O}$  over the southern (northern) region likely yield overestimations (underestimations) of surface uplift, since the topography effect is offset by RH and amount effects. Projecting our modelling results to each locality where paleoelevation studies have been published (Table 4) reveals that topography change explains simulated total isotopic change reasonably well for only few locations (Linzhou Basin, Lunpola Basin, Kailas Basin, Huaitoutala). Indeed topography appears to be the main controlling factor for only 40% of the sites, while 30% are dominated by RH effects, 20% by residual effects and 5% and 5% by post-condensational and non-adiabatic temperature changes, respectively. Nevertheless such figures have to be taken carefully, since we ran idealized experiments testing only the impact of uplift, neglecting other factors like horizontal paleogeography or  $\text{pCO}_2$  variations, the latter being known to influence  $\delta^{18}\text{O}$  as well (Jeffery et al., 2012; Poulsen and Jeffery, 2011).

For the initial uplift stage apparent consistency occurs between the topography impact and the total isotopic composition is observed, in relation with counteracting

effects RH and pots-condensational processes. For the southern region RH impact is appeared to be the main controlling factor for the isotopic composition of precipitation, surpassing the direct topography impact. Nevertheless, these processes have a different contribution for initial and terminal stages of uplift. Precipitation changes lead to overestimate altitude changes for both stages, but for the terminal stage its contribution is bigger. This effect dominates in the southern part, and more generally where the isotopic composition of precipitation strongly depends on convective activity. RH changes dominate over the western part of TP and Northern India for initial uplift stage and over the northern TP for the terminal. Differences between both stages could be partly explained by non-linearities in qs-temperature relationships, as well as in Rayleigh distillation processes. Determining whether other processes contribute to this difference would be of interest, but was out of the scope of the present-study.

## 5 Conclusions

Previous studies focusing on the Andes (Ehlers and Poulsen, 2009; Poulsen et al., 2010) or north American cordillera (Sewall and Fricke, 2013) have inferred that the impact of uplift of mountain ranges on  $\delta^{18}\text{O}$  could be altered by the consequences of the uplift on atmospheric physics and dynamics. Our modelling results show that it is also the case for the Tibetan Plateau uplift. Additionally, we designed a decomposing analysis to quantify for the first time the different processes that can alter precipitation  $\delta^{18}\text{O}$  changes with uplift. As suggested for the Andes, the onset of convective rainfall plays an important role in shifting  $\delta^{18}\text{O}$  towards more negative values. Nevertheless this process is not the main factor, as we show that saturation of air masses, quantified by RH have two to three-time bigger effects on the final  $\delta^{18}\text{O}$ . We infer that increase in precipitation linked with the TP uplift would lead to overestimation of the topography uplift at sites over Himalayas and Southern TP, whereas increase in RH leads to underestimating the uplift at sites in Northern Tibet.

Our results could be applied to interpret paleoclimate records and to reconstruct the region uplift history. Paleoelevation reconstructions suggest the Himalayas attained their current elevation by at least by the late Miocene or even earlier

(Garzione et al., 2000a, 2000b; Rowley et al., 2001; Saylor et al., 2009). Our results show overestimation of the topography impact over this region, thus the Himalayas may have attained their current elevation later than expected. In contrast, isotope-based paleoaltimetry could underestimate surface elevation over the northern TP. This could explain why available isotope-based paleoelevation estimates for the northern TP (Cyr et al., 2005), which estimates surface elevation about 2km, contradict palynological assemblages in lacustrine sediments from the Xining Basin, which show the presence of high-altitude vegetation at the same time period (Dupont-Nivet et al., 2008; Hoorn et al., 2012).

Still, our decomposition methods reveal that even if the impact of the TP uplift phases are rather straightforward (monsoon enhancement to the South, increase in continental recycling over TP, moisture fluxes deflection and increased aridity to the North), the consequences in terms of  $\delta^{18}\text{O}$  are extremely complex, since interplays and compensation occur amongst all the processes. Limitations in our approach are related to ~~a perfectible hydrological cycle in LMDZ-iso, and the theoretical uplift scenario we chose~~ the idealized boundary conditions (topography uplift scenarios, modern land-sea mask, SSTs and  $\text{pCO}_2$ ). Model-data comparison show that mean annual precipitation amount is slightly overestimated by the model for the northern TP, thus could result in underestimation of the amount effect contribution for the northern TP. On the contrary, the model overestimates the precipitation over the southern edge of Himalayas. If it was more realistic, the contribution of the amount effect estimated by the decomposing method could be less important. Changes in vegetation cover, by altering albedo and persistence of snow cover, could affect the impact of non-adiabatic temperature changes on  $\delta^{18}\text{O}$ . Vegetation over Asia was shown to have a major variation through Cenozoic based on pollen (Dupont-Nivet et al., 2008; Miao et al., 2011; Song et al., 2010; Zhao and Yu, 2012) and paleobotanical data (An et al., 2005; De Franceschi et al., 2008; Kohn, 2010) and future studies would benefit to explore its impact on precipitation  $\delta^{18}\text{O}$ . Also it is largely known that during the Cenozoic air temperature was higher due to higher concentration of greenhouse gases in the atmosphere (Zachos et al., 2008). Studies taking into account this feedback inferred that it could lead to even larger inaccuracy in surface uplift estimations during the Cenozoic (Poulsen and Jeffery, 2011). Thus the field of

paleoaltimetry would benefit from future studies focusing on (1) using paleoclimate proxies to constrain specifically relative humidity, surface temperature and precipitation amount in deep time and (2) applying a decomposition method to isotope-enabled GCM simulations forced by constrained paleogeography (land-sea mask and different scenarios for orogens) and atmospheric pCO<sub>2</sub> for specific geological time period. The combination of both could help refining calibration for paleo  $\delta^{18}\text{O}$ -elevation relationships and refining paleoelevation estimates.

## Acknowledgements

This work is a part of iTECC (interaction Tectonics-Erosion-Climate-Coupling) project funded by European Union. Computational resources were provided by IDRIS-GENCI (project 0292), France

## References

- An, Z., Kutzbach, J. E., Prell, W. L. and Porter, S. C.: Evolution of Asian monsoons and phased uplift of the Himalaya-Tibetan plateau since Late Miocene times., *Nature*, 411(6833), 62–66, doi:10.1038/35075035, 2001.
- An, Z., Huang, Y., Liu, W., Guo, Z., Stevens, C., Li, L., Prell, W., Ning, Y., Cai, Y., Zhou, W., Lin, B., Zhang, Q., Cao, Y., Qiang, X., Chang, H. and Wu, Z.: Multiple expansions of C4 plant biomass in East Asia since 7 Ma coupled with strengthened monsoon circulation, *Geology*, 33(9), 705, doi:10.1130/G21423.1, 2005.
- An, Z., Wu, G., Li, J., Sun, Y., Liu, Y., Zhou, W., Cai, Y., Duan, A., Li, L., Mao, J., Cheng, H., Shi, Z., Tan, L., Yan, H., Ao, H., Chang, H. and Feng, J.: Global Monsoon Dynamics and Climate Change, *Annu. Rev. Earth Planet. Sci.*, 43(1), 29–77, doi:10.1146/annurev-earth-060313-054623, 2015.
- Battisti, D. S., Ding, Q. and Roe, G. H.: Coherent pan-Asian climatic and isotopic response to orbital forcing of tropical insolation, *J. Geophys. Res. Atmos.*, 119(21), 11997–12020, doi:10.1002/2014JD021960, 2014.
- Bershaw, J., Penny, S. M. and Garzione, C. N.: Stable isotopes of modern water across the Himalaya and eastern Tibetan Plateau: Implications for estimates of paleoelevation and paleoclimate, *J. Geophys. Res. Atmos.*, 117(2), 1–18, doi:10.1029/2011JD016132, 2012.

1 Boos, W. R. (yale): A review of recent progress on Tibet's role in the South Asian  
2 monsoon, *Clivar*, (1996), 2015.

3 Broccoli, A. J. and Manabe, S.: The Effects of Orography on Midlatitude Northern  
4 Hemisphere Dry Climates, *J. Clim.*, 5(11), 1181–1201, doi:10.1175/1520-  
5 0442(1992)005<1181:teoom>2.0.co;2, 1992.

6 Caves, J. K., Winnick, M. J., Graham, S. A., Sjostrom, D. J., Mulch, A. and Chamberlain, C.  
7 P.: Role of the westerlies in Central Asia climate over the Cenozoic, *Earth Planet. Sci.*  
8 *Lett.*, 428, 33–43, 2015.

9 Chen, B., Xu, X. De, Yang, S. and Zhang, W.: On the origin and destination of  
10 atmospheric moisture and air mass over the Tibetan Plateau, *Theor. Appl. Climatol.*,  
11 110(3), 423–435, doi:10.1007/s00704-012-0641-y, 2012.

12 Chen, G.-S., Liu, Z. and Kutzbach, J. E.: Reexamining the barrier effect of the Tibetan  
13 Plateau on the South Asian summer monsoon, *Clim. Past*, 10(3), 1269–1275,  
14 doi:10.5194/cp-10-1269-2014, 2014.

15 Clift, P. D., Hodges, K. V., Heslop, D., Hannigan, R., Van Long, H. and Calves, G.:  
16 Correlation of Himalayan exhumation rates and Asian monsoon intensity, *Nat.*  
17 *Geosci.*, 1(12), 875–880, doi:10.1038/ngeo351, 2008.

18 Currie, B. S., Rowley, D. B. and Tabor, N. J.: Middle Miocene paleoaltimetry of  
19 southern Tibet: Implications for the role of mantle thickening and delamination in  
20 the Himalayan orogen, *Geology*, 33(3), 181–184, doi:10.1130/G21170.1, 2005.

21 Cyr, A. J., Currie, B. S. and Rowley, D. B.: Geochemical Evaluation of Fenghuoshan  
22 Group Lacustrine Carbonates, North-Central Tibet: Implications for the  
23 Paleoaltimetry of the Eocene Tibetan Plateau, *J. Geol.*, 113(5), 517–533,  
24 doi:10.1086/431907, 2005.

25 Dansgaard, W.: Stable isotopes in precipitation, *Tellus A*,  
26 doi:10.3402/tellusa.v16i4.8993, 1964.

27 DeCelles, P. G., Quade, J., Kapp, P., Fan, M., Dettman, D. L. and Ding, L.: High and dry in  
28 central Tibet during the Late Oligocene, *Earth Planet. Sci. Lett.*, 253(3-4), 389–401,  
29 doi:10.1016/j.epsl.2006.11.001, 2007.

30 Dettman, D. L., Fang, X., Garzione, C. N. and Li, J.: Uplift-driven climate change at 12  
31 Ma: A long  $\delta^{18}\text{O}$  record from the NE margin of the Tibetan plateau, *Earth Planet. Sci.*  
32 *Lett.*, 214(1-2), 267–277, doi:10.1016/S0012-821X(03)00383-2, 2003.



1 Ding, L., Xu, Q., Yue, Y., Wang, H., Cai, F. and Li, S.: The Andean-type Gangdese  
2 Mountains: Paleoelevation record from the Paleocene-Eocene Linzhou Basin, Earth  
3 Planet. Sci. Lett., 392, 250–264, doi:10.1016/j.epsl.2014.01.045, 2014.

4 Dupont-Nivet, G., Hoom, C. and Konert, M.: Tibetan uplift prior to the Eocene-  
5 Oligocene climate transition: Evidence from pollen analysis of the Xining Basin,  
6 Geology, 36(12), 987–990, doi:10.1130/G25063A.1, 2008.

7 Ehlers, T. A. and Poulsen, C. J.: Influence of Andean uplift on climate and  
8 paleoaltimetry estimates, Earth Planet. Sci. Lett., 281(3-4), 238–248,  
9 doi:10.1016/j.epsl.2009.02.026, 2009.

10 Forest, C. E., Wolfe, J. A., Molnar, P. and Emanuel, K. A.: Paleoaltimetry incorporating  
11 atmospheric physics and botanical estimates of paleoclimate, Geol. Soc. Am. Bull.,  
12 111(4), 497–511, doi:10.1130/0016-7606(1999)111<0497:PIAPAB>2.3.CO;2, 1999.

13 De Franceschi, D., Hoorn, C., Antoine, P. O., Cheema, I. U., Flynn, L. J., Lindsay, E. H.,  
14 Marivaux, L., Métais, G., Rajpar, A. R. and Welcomme, J. L.: Floral data from the mid-  
15 Cenozoic of central Pakistan, Rev. Palaeobot. Palynol., 150, 115–129,  
16 doi:10.1016/j.revpalbo.2008.01.011, 2008.

17 Frankenberg, C., Yoshimura, K., Warneke, T., Aben, I., Butz, A., Deutscher, N., Griffith,  
18 D., Hase, F., Notholt, J., Schneider, M., Schrijver, H. and Röckmann, T.: Dynamic  
19 Processes Governing Lower-Tropospheric HDO/H<sub>2</sub>O Ratios as Observed from Space  
20 and Ground, Science (80-. ), 325(5946), 1374–1377, doi:10.1126/science.1173791,  
21 2009.

22 Galewsky, J. and Hurley, J. V: An advection-condensation model for subtropical  
23 water vapor isotopic ratios, J. Geophys. Res. Atmos., 115(D16), 2010.

24 Galewsky, J., Sobel, A. and Held, I.: Diagnosis of subtropical humidity dynamics using  
25 tracers of last saturation, J. Atmos. Sci., 62(9), 3353–3367, 2005.

26 Garzione, C. N., Dettman, D. L., Quade, J., De Celles, P. G. and Butler, R. F.: High times  
27 on the Tibetan Plateau: Paleoelevation of the Thakkhola graben, Nepal, Geology,  
28 28(4), 339–342, doi:10.1130/0091-7613(2000)28<339:HTOTTP>2.0.CO;2, 2000a.

29 Garzione, C. N., Quade, J., DeCelles, P. G. and English, N. B.: Predicting paleoelevation  
30 of Tibet and the Himalaya from  $\delta^{18}\text{O}$  vs. altitude gradients in meteoric water across  
31 the Nepal Himalaya, Earth Planet. Sci. Lett., 183(1-2), 215–229, doi:10.1016/S0012-  
32 821X(00)00252-1, 2000b.

1 Gat, J. R.: Oxygen and hydrogen isotopes in the hydrologic cycle, *Annu. Rev. Earth*  
2 *Planet. Sci.*, 24(1), 225–262, 1996.

3 Gedzelman, S. D. and Arnold, R.: Modeling the isotopic composition of precipitation,  
4 New York, 99, 1994.

5 Gonfiantini, R., Roche, M. A., Olivry, J. C., Fontes, J. C. and Zuppi, G. M.: The altitude  
6 effect on the isotopic composition of tropical rains, *Chem. Geol.*, 181(1-4), 147–167,  
7 doi:10.1016/S0009-2541(01)00279-0, 2001.

8 Guo, Z. T., Ruddiman, W. F., Hao, Q. Z., Wu, H. B., Qiao, Y. S., Zhu, R. X., Peng, S. Z., Wei,  
9 J. J., Yuan, B. Y. and Liu, T. S.: Onset of Asian desertification by 22 Myr ago inferred  
10 from loess deposits in China., *Nature*, 416(6877), 159–163, doi:10.1038/416159a,  
11 2002.

12 Guo, Z. T., Sun, B., Zhang, Z. S., Peng, S. Z., Xiao, G. Q., Ge, J. Y., Hao, Q. Z., Qiao, Y. S.,  
13 Liang, M. Y., Liu, J. F., Yin, Q. Z. and Wei, J. J.: A major reorganization of Asian climate  
14 by the early Miocene, *Clim. Past*, 4(3), 153–174, doi:10.5194/cp-4-153-2008, 2008.

15 Harris, N.: The elevation history of the Tibetan Plateau and its implications for the  
16 Asian monsoon, *Palaeogeogr. Palaeoclimatol. Palaeoecol.*, 241(1), 4–15,  
17 doi:10.1016/j.palaeo.2006.07.009, 2006a.

18 Harris, N.: The elevation history of the Tibetan Plateau and its implications for the  
19 Asian monsoon, *Palaeogeogr. Palaeoclimatol. Palaeoecol.*, 241(1), 4–15,  
20 doi:10.1016/j.palaeo.2006.07.009, 2006b.

21 He, Y., Risi, C., Gao, J., Masson-delmotte, V., Yao, T., Lai, C., Ding, Y., Worden, J.,  
22 Frankenberg, C., Chepfer, H. and Cesana, G.: Special Section : Impact of atmospheric  
23 convection on south Tibet summer precipitation isotopologue composition using a  
24 combination of in situ measurements, satellite data, and atmospheric general  
25 circulation modeling, , 3852–3871, doi:10.1002/2014JD022180.Abstract, 2015.

26 Hoke, G. D., Liu-Zeng, J., Hren, M. T., Wissink, G. K. and Garzzone, C. N.: Stable isotopes  
27 reveal high southeast Tibetan Plateau margin since the Paleogene, *Earth Planet. Sci.*  
28 *Lett.*, 394, 270–278, doi:10.1016/j.epsl.2014.03.007, 2014.

29 Hoorn, C., Straathof, J., Abels, H. a., Xu, Y., Utescher, T. and Dupont-Nivet, G.: A late  
30 Eocene palynological record of climate change and Tibetan Plateau uplift (Xining  
31 Basin, China), *Palaeogeogr. Palaeoclimatol. Palaeoecol.*, 344-345, 16–38,  
32 doi:10.1016/j.palaeo.2012.05.011, 2012.

1 Hourdin, F., Musat, I., Bony, S., Braconnot, P., Codron, F., Dufresne, J. L., Fairhead, L.,  
2 Filiberti, M. A., Friedlingstein, P., Grandpeix, J. Y., Krinner, G., LeVan, P., Li, Z. X. and  
3 Lott, F.: The LMDZ4 general circulation model: Climate performance and sensitivity  
4 to parametrized physics with emphasis on tropical convection, *Clim. Dyn.*, 27(7-8),  
5 787–813, doi:10.1007/s00382-006-0158-0, 2006.

6 Hren, M. T., Bookhagen, B., Blisniuk, P. M., Booth, A. L. and Chamberlain, C. P.:  $\delta^{18}\text{O}$   
7 and  $\delta\text{D}$  of streamwaters across the Himalaya and Tibetan Plateau: Implications for  
8 moisture sources and paleoelevation reconstructions, *Earth Planet. Sci. Lett.*, 288(1-  
9 2), 20–32, doi:10.1016/j.epsl.2009.08.041, 2009.

10 Jeffery, M. L., Poulsen, C. J. and Ehlers, T. A.: Impacts of Cenozoic global cooling,  
11 surface uplift, and an inland seaway on South American paleoclimate and  
12 precipitation  $\delta^{18}\text{O}$ , *Geol. Soc. Am. Bull.*, 124(3-4), 335–351, 2012.

13 Kageyama, M., Nebout, N. C., Sepulchre, P., Peyron, O., Krinner, G., Ramstein, G. and  
14 Cazet, J.-P.: The Last Glacial Maximum and Heinrich Event 1 in terms of climate and  
15 vegetation around the Alboran Sea: a preliminary model-data comparison, *Comptes*  
16 *Rendus Geosci.*, 337(10-11), 983–992, doi:10.1016/j.crte.2005.04.012, 2005.

17 Kanamitsu, M., Ebisuzaki, W., Woollen, J., Yang, S. K., Hnilo, J. J., Fiorino, M. and  
18 Potter, G. L.: NCEP-DOE AMIP-II reanalysis (R-2), *Bull. Am. Meteorol. Soc.*, 83(11),  
19 1631–1643+1559, doi:10.1175/BAMS-83-11-1631, 2002.

20 Kattel, D. B., Yao, T., Yang, W., Gao, Y. and Tian, L.: Comparison of temperature lapse  
21 rates from the northern to the southern slopes of the Himalayas, *Int. J. Climatol.*,  
22 2015.

23 Khan, M. A., Spicer, R. a., Bera, S., Ghosh, R., Yang, J., Spicer, T. E. V, Guo, S. X., Su, T.,  
24 Jacques, F. and Grote, P. J.: Miocene to Pleistocene floras and climate of the Eastern  
25 Himalayan Siwaliks, and new palaeoelevation estimates for the Namling-Oiyug  
26 Basin, Tibet, *Glob. Planet. Change*, 113, 1–10, doi:10.1016/j.gloplacha.2013.12.003,  
27 2014.

28 Kohn, M. J.: Carbon isotope compositions of terrestrial C3 plants as indicators of  
29 (paleo)ecology and (paleo)climate, *Proc. Natl. Acad. Sci.*, 107(46), 19691–19695,  
30 doi:10.1073/pnas.1004933107, 2010.

31 Kutzbach, J. E., Guetter, P. J., Ruddiman, W. F. and Prell, W. L.: Sensitivity of climate to  
32 late Cenozoic uplift in southern Asia and the American west: numerical experiments,

1 J. Geophys. Res. Atmos., 94(D15), 18393–18407, 1989.

2 Kutzbach, J. E., Prell, W. L. and Ruddiman, W. F.: Sensitivity of Eurasian climate to  
3 surface uplift of the Tibetan Plateau, J. Geol., 177–190, 1993.

4 Ladant, J., Donnadieu, Y., Lefebvre, V. and Dumas, C.: The respective role of  
5 atmospheric carbon dioxide and orbital parameters on ice sheet evolution at the  
6 Eocene-Oligocene transition, Paleoclimatology, 29(8), 810–823,  
7 doi:10.1002/2013PA002593, 2014.

8 Lee, J. and Fung, I.: “Amount effect” of water isotopes and quantitative analysis of  
9 post-condensation processes, Hydrol. Process., 22(1), 1–8, 2008.

10 Lee, J. E., Risi, C., Fung, I., Worden, J., Scheepmaker, R. A., Lintner, B. and  
11 Frankenberg, C.: Asian monsoon hydrometeorology from TES and SCIAMACHY  
12 water vapor isotope measurements and LMDZ simulations: Implications for  
13 speleothem climate record interpretation, J. Geophys. Res. Atmos., 117(15), 1–12,  
14 doi:10.1029/2011JD017133, 2012.

15 Van Leer, B.: Towards the ultimate conservative difference scheme. IV. A new  
16 approach to numerical convection, J. Comput. Phys., 23(3), 276–299,  
17 doi:http://dx.doi.org/10.1016/0021-9991(77)90095-X, 1977.

18 LeGrande, A. N. and Schmidt, G. A.: Sources of Holocene variability of oxygen  
19 isotopes in paleoclimate archives, Clim. Past, 5(3), 441–455, doi:10.5194/cp-5-441-  
20 2009, 2009.

21 Li, S., Currie, B. S., Rowley, D. B. and Ingalls, M.: Cenozoic paleoaltimetry of the SE  
22 margin of the Tibetan Plateau: Constraints on the tectonic evolution of the region,  
23 Earth Planet. Sci. Lett., 432, 415–424, doi:10.1016/j.epsl.2015.09.044, 2015.

24 Licht, A., van Cappelle, M., Abels, H. A., Ladant, J.-B., Trabucho-Alexandre, J., France-  
25 Lanord, C., Donnadieu, Y., Vandenberghe, J., Rigaudier, T., Lécuyer, C., Terry Jr, D.,  
26 Adriaens, R., Boura, A., Guo, Z., Soe, A. N., Quade, J., Dupont-Nivet, G. and Jaeger, J.-J.:  
27 Asian monsoons in a late Eocene greenhouse world, Nature, 513(7519), 501–506,  
28 doi:10.1038/nature13704, 2014.

29 Liu, X., Sun, H., Miao, Y., Dong, B. and Yin, Z.-Y.: Impacts of uplift of northern Tibetan  
30 Plateau and formation of Asian inland deserts on regional climate and environment,  
31 Quat. Sci. Rev., 116, 1–14, doi:10.1016/j.quascirev.2015.03.010, 2015.

32 McElwain, J. C.: Climate-independent paleoaltimetry using stomatal density in fossil

1 leaves as a proxy for CO<sub>2</sub> partial pressure, *Geology*, 32(12), 1017,  
2 doi:10.1130/G20915.1, 2004.

3 Merlivat, L. and Nief, G.: Fractionnement isotopique lors des changements d'état  
4 solide-vapeur et liquide-vapeur de l'eau à des températures inférieures à 0°C, *Tellus*,  
5 19(1), 122–127, doi:10.1111/j.2153-3490.1967.tb01465.x, 1967.

6 Miao, Y., Fang, X., Herrmann, M., Wu, F., Zhang, Y. and Liu, D.: Miocene pollen record  
7 of KC-1 core in the Qaidam Basin, NE Tibetan Plateau and implications for evolution  
8 of the East Asian monsoon, *Palaeogeogr. Palaeoclimatol. Palaeoecol.*, 299(1-2), 30–  
9 38, doi:10.1016/j.palaeo.2010.10.026, 2011.

10 Miao, Y., Herrmann, M., Wu, F., Yan, X. and Yang, S.: What controlled Mid-Late  
11 Miocene long-term aridification in Central Asia? - Global cooling or Tibetan Plateau  
12 uplift: A review, *Earth-Science Rev.*, 112(3-4), 155–172,  
13 doi:10.1016/j.earscirev.2012.02.003, 2012.

14 Molnar, P., Boos, W. R. and Battisti, D. S.: Orographic Controls on Climate and  
15 Paleoclimate of Asia: Thermal and Mechanical Roles for the Tibetan Plateau, *Annu.*  
16 *Rev. Earth Planet. Sci.*, 38(1), 77–102, doi:10.1146/annurev-earth-040809-152456,  
17 2010.

18 Mulch, A.: Stable isotope paleoaltimetry and the evolution of landscapes and life,  
19 *Earth Planet. Sci. Lett.*, 433, 180–191, doi:10.1016/j.epsl.2015.10.034, 2016.

20 New, M., Lister, D., Hulme, M. and Makin, I.: A high-resolution data set of surface  
21 climate over global land areas, *Clim. Res.*, 21(1), 1–25, doi:10.3354/cr021001, 2002.

22 Pausata, F. S. R., Battisti, D. S., Nisancioglu, K. H. and Bitz, C. M.: Chinese stalagmite  
23  $\delta^{18}\text{O}$  controlled by changes in the Indian monsoon during a simulated Heinrich  
24 event, *Nat. Geosci.*, 4(7), 474–480, doi:10.1038/ngeo1169, 2011.

25 Poage, M. A. and Chamberlain, C. P.: Empirical relationships between elevation and  
26 the stable isotope composition of precipitation and surface waters: Considerations  
27 for studies of paleoelevation change, *Am. J. Sci.*, 301(1), 1–15,  
28 doi:10.2475/ajs.301.1.1, 2001.

29 Pohl, A., Donnadieu, Y., Le Hir, G., Buoncristiani, J.-F. and Vennin, E.: Effect of the  
30 Ordovician paleogeography on the (in)stability of the climate, *Clim. Past*, 10(6),  
31 2053–2066, doi:10.5194/cp-10-2053-2014, 2014.

32 Poulsen, C. J. and Jeffery, M. L.: Climate change imprinting on stable isotopic

1 compositions of high-elevation meteoric water cloaks past surface elevations of  
2 major orogens, *Geology*, 39(6), 595–598, doi:10.1130/G32052.1, 2011.

3 Poulsen, C. J., Ehlers, T. a and Insel, N.: Onset of convective rainfall during gradual  
4 late Miocene rise of the central Andes., *Science*, 328(5977), 490–493,  
5 doi:10.1126/science.1185078, 2010.

6 Quade, J., Garzione, C. and Eiler, J.: Paleoelevation Reconstruction using Pedogenic  
7 Carbonates, *Rev. Mineral. Geochemistry*, 66(1), 53–87, doi:10.2138/rmg.2007.66.3,  
8 2007.

9 Quade, J., Breecker, D. O., Daëron, M. and Eiler, J.: The paleoaltimetry of Tibet: An  
10 isotopic perspective, *Am. J. Sci.*, 311(2), 77–115, doi:10.2475/02.2011.01, 2011.

11 Ramstein, G., Fluteau, F., Besse, J. and Joussaume, S.: Effect of orogeny, plate motion  
12 and land–sea distribution on Eurasian climate change over the past 30 million years,  
13 *Nature*, 386(6627), 788–795, doi:10.1038/386788a0, 1997.

14 Raymo, M. E. and Ruddiman, W. F.: Tectonic forcing of late Cenozoic climate, *Nature*,  
15 359(6391), 117–122, 1992.

16 Risi, C., Bony, S. and Vimeux, F.: Influence of convective processes on the isotopic  
17 composition ( $\delta^{18}\text{O}$  and  $\delta\text{D}$ ) of precipitation and water vapor in the tropics: 2.  
18 Physical interpretation of the amount effect, *J. Geophys. Res. Atmos.*, 113(19), 1–12,  
19 doi:10.1029/2008JD009943, 2008.

20 Risi, C., Bony, S., Vimeux, F. and Jouzel, J.: Water-stable isotopes in the LMDZ4  
21 general circulation model: Model evaluation for present-day and past climates and  
22 applications to climatic interpretations of tropical isotopic records, *J. Geophys. Res.*  
23 *Atmos.*, 115(12), 1–27, doi:10.1029/2009JD013255, 2010.

24 Risi, C., Noone, D., Frankenberg, C. and Worden, J.: Role of continental recycling in  
25 intraseasonal variations of continental moisture as deduced from model simulations  
26 and water vapor isotopic measurements, *Water Resour. Res.*, 49(7), 4136–4156,  
27 doi:10.1002/wrcr.20312, 2013.

28 Rodwell, M. J. and Hoskins, B. J.: Subtropical anticyclones and summer monsoons, *J.*  
29 *Clim.*, 14(15), 3192–3211, 2001.

30 Rowley, D. B. and Currie, B. S.: Palaeo-altimetry of the late Eocene to Miocene  
31 Lunpola basin, central Tibet., *Nature*, 439(7077), 677–681,  
32 doi:10.1038/nature04506, 2006.

1 Rowley, D. B. and Garzzone, C. N.: Stable Isotope-Based Paleoaltimetry, *Annu. Rev.*  
2 *Earth Planet. Sci.*, 35(1), 463–508, doi:10.1146/annurev.earth.35.031306.140155,  
3 2007.

4 Rowley, D. B., Pierrehumbert, R. T. and Currie, B. S.: A new approach to stable  
5 isotope-based paleoaltimetry: Implications for paleoaltimetry and paleohypsometry  
6 of the High Himalaya since the late Miocene, *Earth Planet. Sci. Lett.*, 188(1-2), 253–  
7 268, doi:10.1016/S0012-821X(01)00324-7, 2001.

8 Royden, L. H., Burchfiel, B. C. and Hilst, R. D. Van Der: The Geological Evolution of the  
9 Tibetan Plateau, , 321(August), 1054–1058, 2008.

10 Rozanski, Kazimierz Araguás-Araguás, L. and Gonfiantini, R.: Isotopic patterns in  
11 modern global precipitation, *Clim. Chang. Cont. Isot. Rec.*, 1–36, 1993.

12 Ruddiman, W. F. and Kutzbach, J. E.: Forcing of late Cenozoic northern hemisphere  
13 climate by plateau uplift in southern Asia and the American West, *J. Geophys. Res.*  
14 *Atmos.*, 94(D15), 18409–18427, 1989.

15 Sato, T. and Kimura, F.: Impact of diabatic heating over the Tibetan Plateau on  
16 subsidence over northeast Asian arid region, *Geophys. Res. Lett.*, 32(5), 1–5,  
17 doi:10.1029/2004GL022089, 2005.

18 Saylor, J. E., Quade, J., Dettman, D. L., DeCelles, P. G., Kapp, P. A. and Ding, L.: The late  
19 Miocene through present paleoelevation history of southwestern Tibet, *Am. J. Sci.*,  
20 309(1), 1–42, doi:10.2475/01.2009.01, 2009.

21 Sepulchre, P., Ramstein, G., Fluteau, F., Schuster, M., Tiercelin, J.-J. and Brunet, M.:  
22 Tectonic uplift and Eastern Africa aridification., *Science*, 313(5792), 1419–1423,  
23 doi:10.1126/science.1129158, 2006.

24 Sewall, J. O. and Fricke, H. C.: Andean-scale highlands in the Late Cretaceous  
25 Cordillera of the North American western margin, *Earth Planet. Sci. Lett.*, 362, 88–  
26 98, doi:10.1016/j.epsl.2012.12.002, 2013.

27 Sherwood, S. C.: Maintenance of the free-tropospheric tropical water vapor  
28 distribution. Part II: Simulation by large-scale advection, *J. Clim.*, 9(11), 2919–2934,  
29 1996.

30 Song, X. Y., Spicer, R. a., Yang, J., Yao, Y. F. and Li, C. Sen: Pollen evidence for an  
31 Eocene to Miocene elevation of central southern Tibet predating the rise of the High  
32 Himalaya, *Palaeogeogr. Palaeoclimatol. Palaeoecol.*, 297(1), 159–168,

1    doi:10.1016/j.palaeo.2010.07.025, 2010.

2    Stowhas, L. and Moyano, J. C.: Simulation of the Isotopic Content of Precipitation,  
3    Atmos. Environ. Part a-General Top., 27(3), 327–333, doi:10.1016/0960-  
4    1686(93)90106-9, 1993.

5    Sun, B., Wang, Y.-F., Li, C.-S., Yang, J., Li, J.-F., Li, Y.-L., Deng, T., Wang, S.-Q., Zhao, M.,  
6    Spicer, R. a., Ferguson, D. K. and Mehrotra, R. C.: Early Miocene elevation in northern  
7    Tibet estimated by palaeobotanical evidence, Sci. Rep., 5(1), 10379,  
8    doi:10.1038/srep10379, 2015.

9    Sun, J., Zhang, Z. and Zhang, L.: New evidence on the age of the Taklimakan Desert,  
10    Geology, 37(2), 159–162, doi:10.1130/G25338A.1, 2009.

11    Sun, J., Xu, Q., Liu, W., Zhang, Z., Xue, L. and Zhao, P.: Palynological evidence for the  
12    latest Oligocene-early Miocene paleoelevation estimate in the Lunpola Basin, central  
13    Tibet, Palaeogeogr. Palaeoclimatol. Palaeoecol., 399, 21–30,  
14    doi:10.1016/j.palaeo.2014.02.004, 2014.

15    Sun, X. and Wang, P.: How old is the Asian monsoon system?—Palaeobotanical  
16    records from China, Palaeogeogr. Palaeoclimatol. Palaeoecol., 222(3–4), 181–222,  
17    doi:http://dx.doi.org/10.1016/j.palaeo.2005.03.005, 2005.

18    Tapponnier, P., Zhiqin, X., Roger, F., Meyer, B., Arnaud, N., Wittlinger, G. and Jingsui,  
19    Y.: Oblique stepwise rise and growth of the Tibet plateau., Science, 294(5547),  
20    1671–1677, doi:10.1126/science.105978, 2001.

21    Taylor, K. E., Williamson, D. and Zwiers, F.: The sea surface temperature and sea-ice  
22    concentration boundary conditions for AMIP II simulations, Program for Climate  
23    Model Diagnosis and Intercomparison, Lawrence Livermore National Laboratory,  
24    University of California., 2000.

25    Tian, L., Yao, T., MacClune, K., White, J. W. C., Schilla, A., Vaughn, B., Vachon, R. and  
26    Ichiyanagi, K.: Stable isotopic variations in west China: A consideration of moisture  
27    sources, J. Geophys. Res. Atmos., 112(10), 1–12, doi:10.1029/2006JD007718, 2007.

28    Vuille, M., Werner, M., Bradley, R. S., Chan, R. Y. and Keimig, F.: Stable isotopes in  
29    East African precipitation record Indian Ocean zonal mode, Geophys. Res. Lett.,  
30    32(21), 1–5, doi:10.1029/2005GL023876, 2005.

31    Xu, Q., Ding, L., Zhang, L., Cai, F., Lai, Q., Yang, D. and Liu-Zeng, J.: Paleogene high  
32    elevations in the Qiangtang Terrane, central Tibetan Plateau, Earth Planet. Sci. Lett.,



362, 31–42, doi:10.1016/j.epsl.2012.11.058, 2013.

Yang, X., Yao, T., Yang, W., Yu, W. and Qu, D.: Co-existence of temperature and amount effects on precipitation  $\delta^{18}\text{O}$  in the Asian monsoon region, *Geophys. Res. Lett.*, 38(November), 1–6, doi:10.1029/2011GL049353, 2011.

Yao, T., Masson-Delmotte, V., Gao, J., Yu, W., Yang, X., Risi, C., Sturm, C., Werner, M., Zhao, H., He, Y., Ren, W., Tian, L., Shi, C. and Hou, S.: A review of climatic controls on  $\delta^{18}\text{O}$  in precipitation over the Tibetan Plateau: Observations and simulations, *Rev. Geophys.*, 51(4), 525–548, doi:10.1002/rog.20023, 2013.

Zachos, J. C., Dickens, G. R. and Zeebe, R. E.: An early Cenozoic perspective on greenhouse warming and carbon-cycle dynamics., *Nature*, 451(7176), 279–283, doi:10.1038/nature06588, 2008.

Zhang, R., Jiang, D., Zhang, Z. and Yu, E.: The impact of regional uplift of the Tibetan Plateau on the Asian monsoon climate, *Palaeogeogr. Palaeoclimatol. Palaeoecol.*, 417, 137–150, doi:10.1016/j.palaeo.2014.10.030, 2015.

Zhang, Z., Wang, H., Guo, Z. and Jiang, D.: What triggers the transition of palaeoenvironmental patterns in China, the Tibetan Plateau uplift or the Paratethys Sea retreat?, *Palaeogeogr. Palaeoclimatol. Palaeoecol.*, 245(3-4), 317–331, doi:10.1016/j.palaeo.2006.08.003, 2007.

Zhao, Y. and Yu, Z.: Vegetation response to Holocene climate change in East Asian monsoon-margin region, *Earth-Science Rev.*, 113(1-2), 1–10, doi:10.1016/j.earscirev.2012.03.001, 2012.

Table 1. Table detailing how the different terms of the decomposition for  $\Delta R_p$ , as written in Eq. (7), are estimated

Term written with differential format	Estimate of these terms	Physical meaning
$\Delta R_p$	$R_p(\delta R_{vi2}, \varepsilon_2, h_2, \delta T_{s2}, z_2) - R_p(\delta R_{vi1}, \varepsilon_1, h_1, \delta T_{s1}, z_1)$	Total isotopic difference between state 1 and state 2
$\Delta R_{p,\Delta z}$	$R_p(\varepsilon', \delta R_v', h', \delta T_s', z_2) - R_p(\varepsilon', \delta R_v', h', \delta T_s', z_1)$	Direct effect of topography change
$\Delta R_{p,\Delta \delta T_s}$	$R_p(\varepsilon', \delta R_v', h', \delta T_{s2}, z') - R_p(\varepsilon', \delta R_v', h', \delta T_{s1}, z')$	Effect of lapse rate change, associated with non-adiabatic effects, possibly due to changes in surface energy budget or in large-scale atmospheric stratification
$\Delta R_{p,\Delta h}$	$R_p(\varepsilon', \delta R_v', h_2, \delta T_s', z') - R_p(\varepsilon', \delta R_v', h_1, \delta T_s', z')$	Effect of local relative humidity change, possibly due to large-scale circulation changes
$\Delta R_{p,\Delta \varepsilon}$	$R_p(\varepsilon_2, \delta R_v', h', \delta T_s', z') - R_p(\varepsilon_1, \delta R_v', h', \delta T_s', z')$	Effect of changes in condensational and post-condensational effects, possibly due to changes in rain reevaporation processes
$\Delta R_{p,\Delta \delta R_v}$	$R_p(\varepsilon', \delta R_{v2}, h', \delta T_s', z') - R_p(\varepsilon', \delta R_{v1}, h', \delta T_s', z')$	All other effects, including effects of deep convection, mixing, water vapour origin, continental recycling on the initial water vapour

Table 2. INT-LOW and MOD-INT sensitivity of the decomposition terms (in ‰) to the changes of  $R_{v0}$ ,  $T_0$ ,  $q_0$ , of 1‰, 1K and 10% respectively.

	Northern Region			South region		
	$T_0$	$q_0$	$R_{v0}$	$T_0$	$q_0$	$R_{v0}$
INT-LOW experiment						
$\Delta R_{p,\Delta z}$	0.08	0.33	0.67	0.07	0.25	0.51
$\Delta R_{p,\Delta \delta T_s}$	0.01	0.02	0.04	0.07	0.06	0.13
$\Delta R_{p,\Delta h}$	0	0.35	0.66	0	0.19	0.83
$\Delta R_{p,\Delta \delta R_{vi}}$	0	0	0.05	0	0	0.52
$\Delta R_{p,\Delta \varepsilon}$	0	0	0	0	0	0
MOD-INT experiment						
$\Delta R_{p,\Delta z}$	0.21	0.6	0.8	0.17	0.59	0.9
$\Delta R_{p,\Delta \delta T_s}$	0.2	0.09	0.18	0.19	0.02	0.05
$\Delta R_{p,\Delta h}$	0	0.58	0.6	0	0.37	0.27
$\Delta R_{p,\Delta \delta R_{vi}}$	0	0	0.65	0	0	0.67
$\Delta R_{p,\Delta \varepsilon}$	0	0	0	0	0	0

Table 3. Values of isotopic changes due to decomposed terms for two uplift stages and for two regions (see the text)

Term	Isotopic change (‰)			
	Initial Stage		Terminal Stage	
	South	North	South	North

$\Delta R_{p,\Delta z}$	-1.40	-2.00	-3.96	-5.50
$\Delta R_{p,\Delta \delta Ts}$	0.4	-0.09	0.76	-0.25
$\Delta R_{p,\Delta h}$	2.40	1.97	1.38	2.50
$\Delta R_{p,\Delta \varepsilon}$	-1.30	-1.73	-0.41	0.01
$\Delta R_{p,\Delta \delta Rv}$	-1.10	-0.14	-2.38	-0.54
Total $\Delta R_p$	-1.00	-1.99	-4.61	-3.16

1  
2  
3



Janggalsay	38.15	86.62	-4.487	-2.406	1.026	-2.347	-0.952	0.192	Kent-Corson et al. (2009)
Jianchuan Basin	26.60	99.80	-1.356	-1.574	0.634	0.171	0.497	-1.083	Hoke et al. (2014)
Jingou	44.75	85.40	1.073	-0.031	1.270	1.435	-2.054	0.453	Charreau et al. (2012)
Kailas Basin	31.20	81.00	-6.705	-7.181	0.401	0.799	3.162	-3.886	DeCelles et al. (2011)
Kuitun	45.00	84.75	1.073	-0.031	1.270	1.435	-2.054	0.453	Charreau et al. (2012)
Lake Mahai	37.66	94.24	-0.964	-0.003	2.737	0.423	-4.188	0.066	Kent-Corson et al. (2009)
Lanping	26.50	99.40	-1.356	-1.574	0.634	0.171	0.497	-1.083	Hoke et al. (2014)
Lao Mangnai	36.94	91.96	-1.133	-3.998	0.447	0.356	2.233	-0.171	Kent-Corson et al. (2009)
Lenghu	37.84	93.36	-0.964	-0.003	2.737	0.423	-4.188	0.066	Kent-Corson et al. (2009)
Linxia Basin	35.69	103.10	0.443	-0.961	1.079	0.364	-0.410	0.371	Dettman et al. (2003)
Linzhou Basin	30.00	91.20	-6.756	-5.956	2.337	-0.057	0.886	-3.965	Ding et al. (2014)
Luhe	25.20	101.30	-0.242	0.009	0.317	0.411	-0.236	-0.742	Hoke et al. (2014)
Lulehe	37.50	95.08	-0.061	-0.987	1.724	1.950	-3.326	0.578	Kent-Corson et al. (2009)
Lulehe	37.50	95.08	-0.061	-0.987	1.724	1.950	-3.326	0.578	Kent-Corson et al. (2009)
Lunpola	32.06	89.75	-6.763	-6.073	1.920	-0.652	1.561	-3.520	Rowley and Currie

Basin									(2006)
									Kent-Corson et al.
Miran River	38.98	88.85	-4.786	-1.387	1.069	-2.683	-2.068	0.283	(2009)
Nepal									
Siwaliks	27.42	82.84	-1.370	0.006	-0.016	0.203	0.025	-1.588	Quade et al. (1995)
Nima Basin	31.75	87.50	-5.897	-7.724	-0.205	1.312	4.078	-3.359	DeCelles et al. (2011)
Oiyug Basin	29.70	89.50	-10.39	-7.842	2.634	-2.598	1.151	-3.735	Currie et al. (2005)
Oytag	38.98	75.51	-0.499	-0.716	1.320	0.719	-1.975	0.152	Bershaw et al. (2011)
Pakistan									
Siwaliks	33.39	73.11	0.645	0.008	0.380	0.407	0.379	-0.529	Quade et al. (1995)
									Kent-Corson et al.
Puska	37.12	78.60	-2.598	0.006	0.896	-0.472	-3.909	0.882	(2009)
Taatsin Gol	45.42	101.26	-0.731	-0.003	1.600	-0.364	-3.087	1.123	Caves et al. (2014)
Thakkhola	28.70	83.50	-4.018	-1.529	0.802	-0.310	-0.572	-2.409	Garziona et al. (2000)
Thakkhola-									
Tetang	28.66	83.50	-4.018	-1.529	0.802	-0.310	-0.572	-2.409	Garziona et al. (2000)
									Kent-Corson et al.
Xiao Qaidam	37.03	94.88	1.614	-1.376	1.772	3.117	-2.581	0.681	(2009)
Xifeng	35.70	107.60	0.245	0.00	0.522	0.173	-0.010	-0.440	Jiang et al. (2002)
									Kent-Corson et al.
Xorkol	39.01	91.92	-3.218	-0.871	1.871	-1.302	-2.970	0.054	(2009)
Xunhua									
Basin	35.90	102.50	0.443	-0.961	1.079	0.364	-0.420	0.371	Hough et al. (2010)

Yanyuan	27.50	101.50	-0.350	-1.152	0.657	0.539	0.373	-0.767	Hoke et al. (2014)
Zhada Basin	31.50	79.75	-3.983	-4.818	-0.046	0.831	2.708	-2.657	Saylor et al. (2009)

1



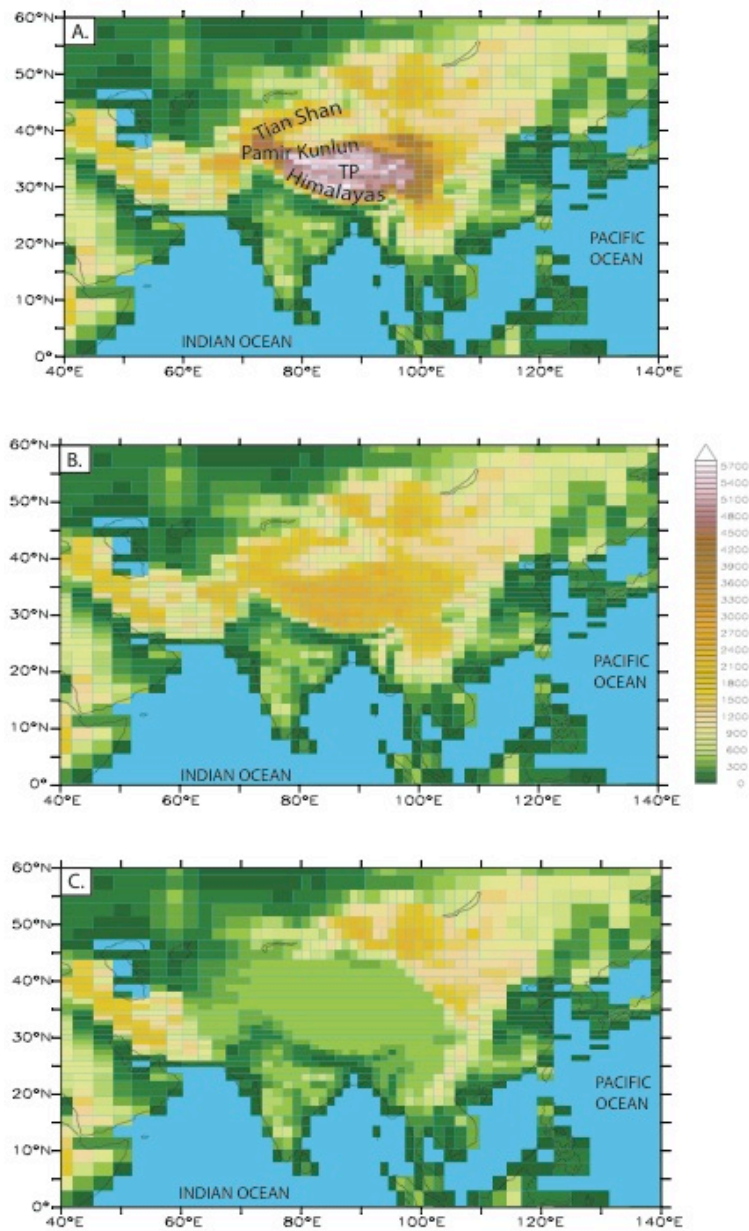


Figure 1. Models design (A) 100% of modern topography - MOD case; (B) Tibetan Plateau, Himalayas, Tian Shan, Pamir, Kunlun and Hindu Kush elevations reduced to 50% of modern elevation - INT case; (C) Tibetan Plateau, Himalayas, Tian Shan, Pamir, Kunlun and Hindu Kush elevations reduced to 250 m - LOW case. **Black rectangles show the division of the TP by regions: southern TP (between 25°N and 30°N), central TP (between 30°N and 35°N) and northern TP (between 35°N and 40°N).**

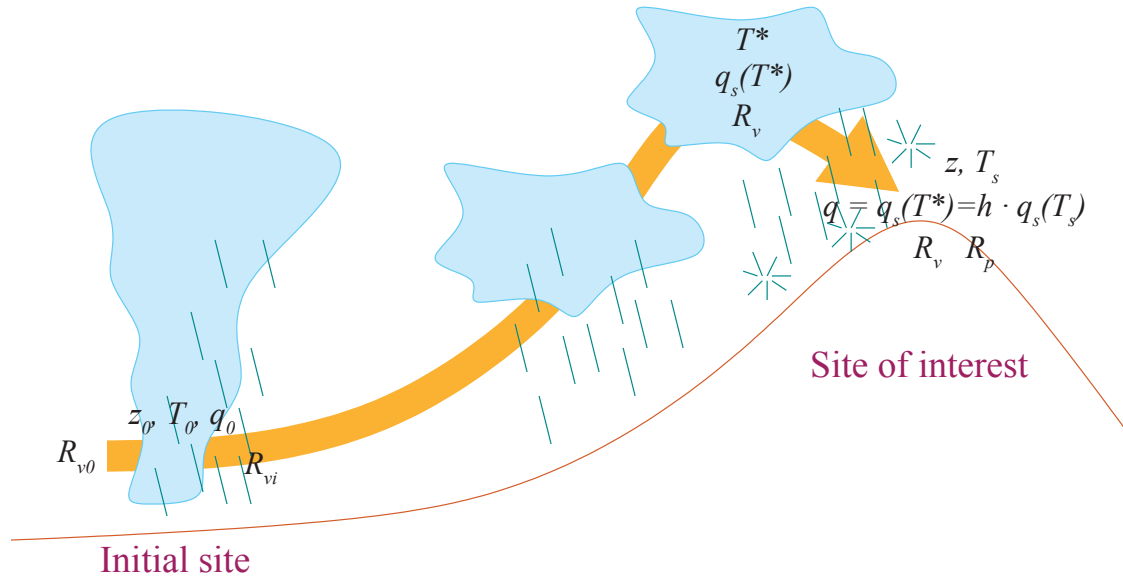


Figure 2. Idealized framework of an isolated air parcel transported from an initial site at low altitude to the site of interest. Most notations are illustrated.

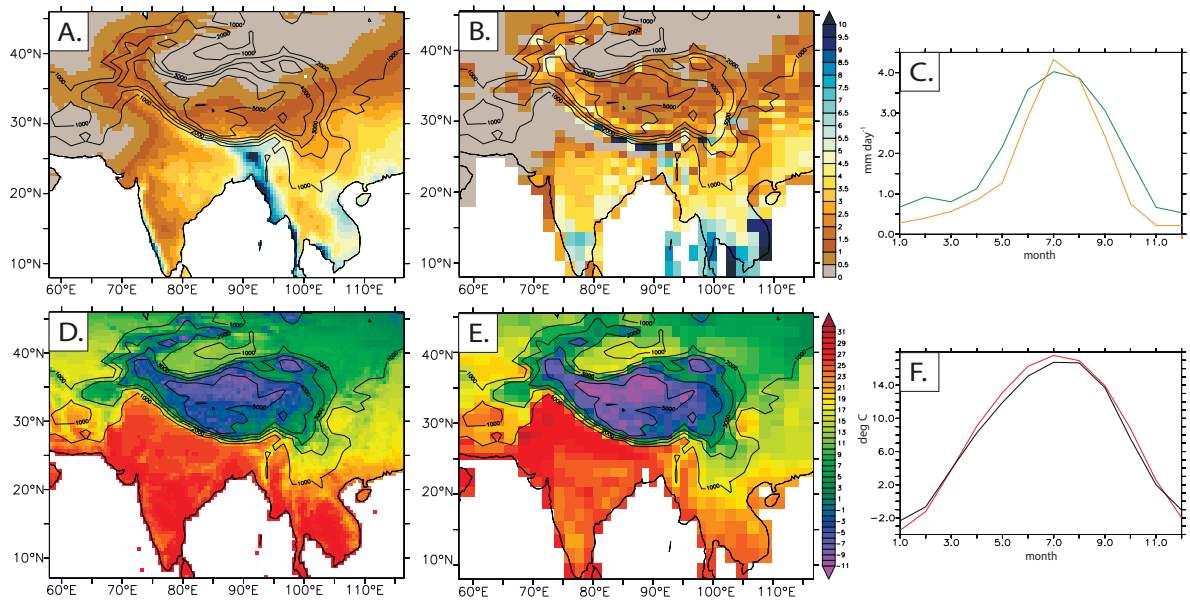


Figure 3. CRU dataset annual-mean rainfall (mm/day) (A) and annual-mean temperature (°C) (D) compared to simulated annual-mean rainfall for MOD experiment

(B) and simulated annual-mean temperature for MOD experiment (E). The seasonal cycles of spatially averaged from 25°N to 40°N and from 75°E to 100°E for the MOD experiment precipitation (C) and temperature (F). Green and red lines of figures (C) and (F) corresponds for MOD experiment, orange and black to the CRU dataset respectively.

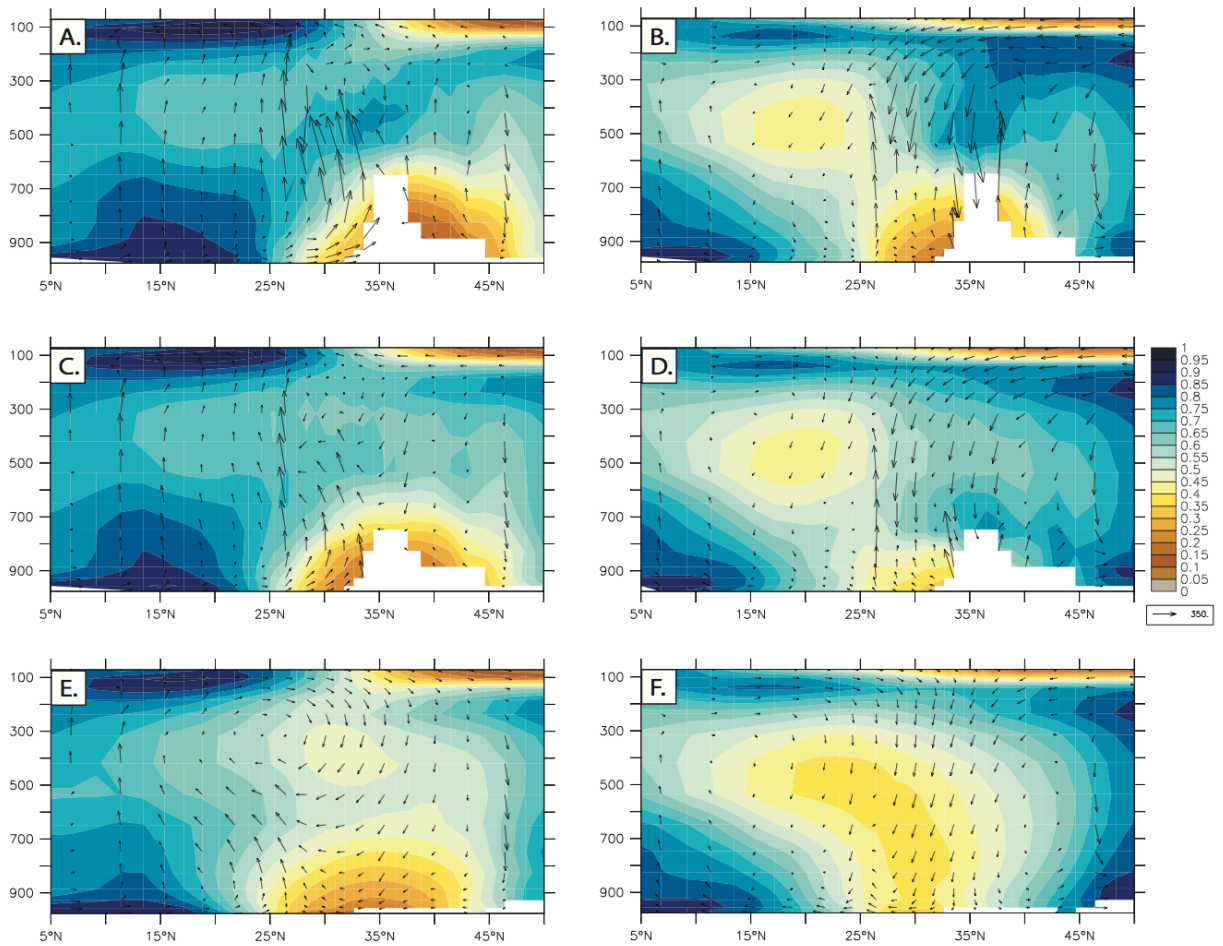


Figure 4. Cross-TP profiles (averaged between 70 and 90°E) showing the relative humidity and moisture transport for seasons (A, C, E) MJJAS and (B, D, F) ONDJFMA and

for 3 simulation: (A, B) MOD, (C, D) INT, (E, F) LOW cases.

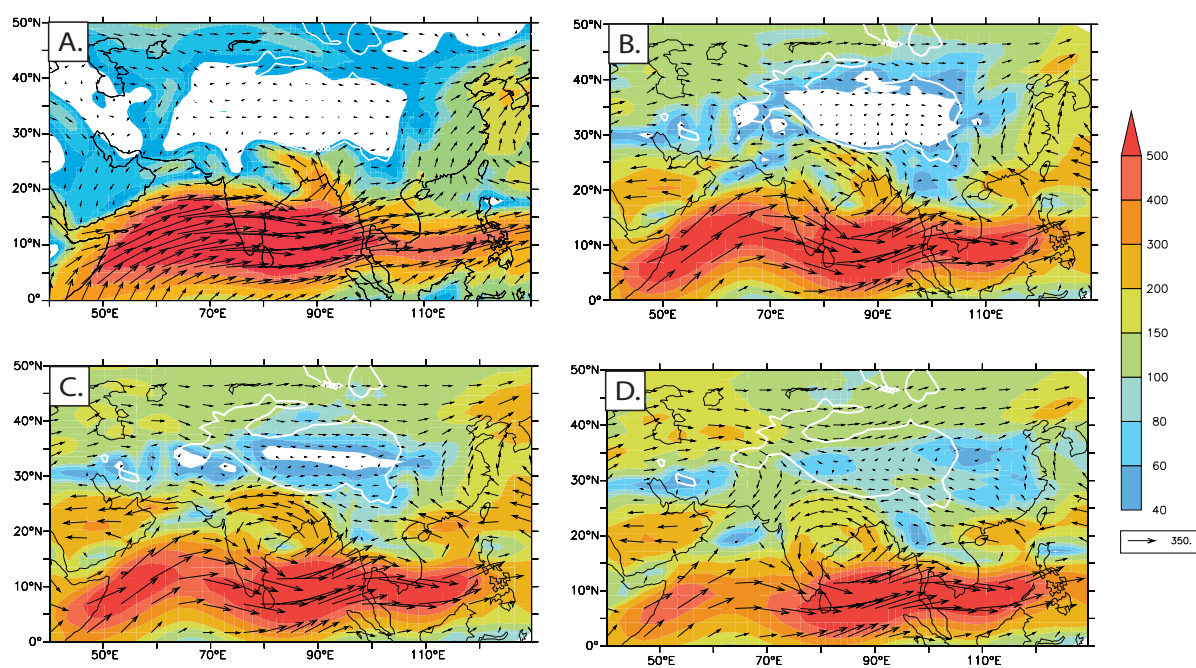


Figure 5. Directions and intensity of JJA vertically-integrated humidity transport for: (A) averaged from ERA-40 re-analysis and for (B) MOD case, (C) INT case, (D) LOW case.

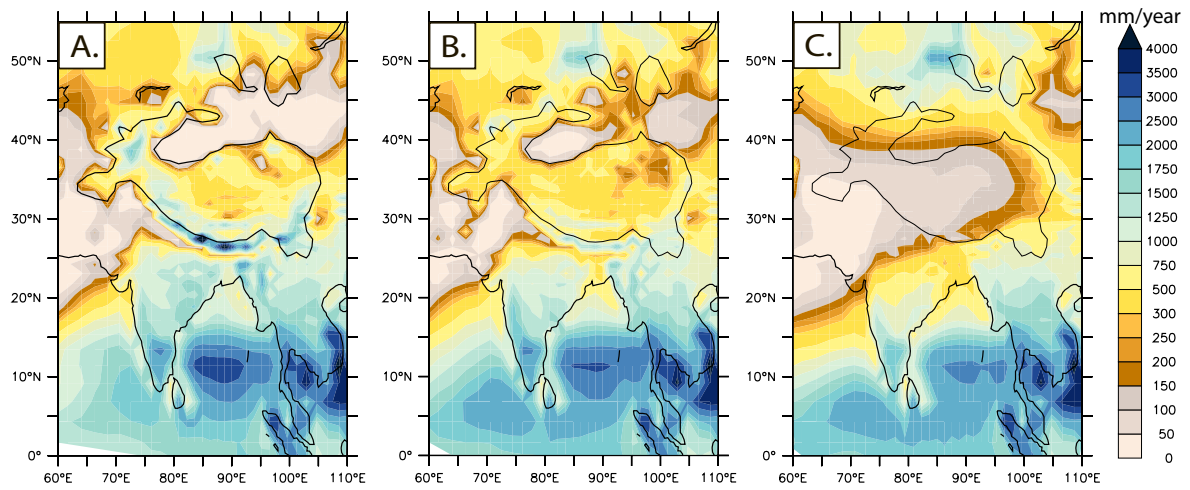


Figure 6. Annual mean precipitation amount (absolute values, mm/year) for: (A) MOD case, (B) INT case, (C) LOW case.

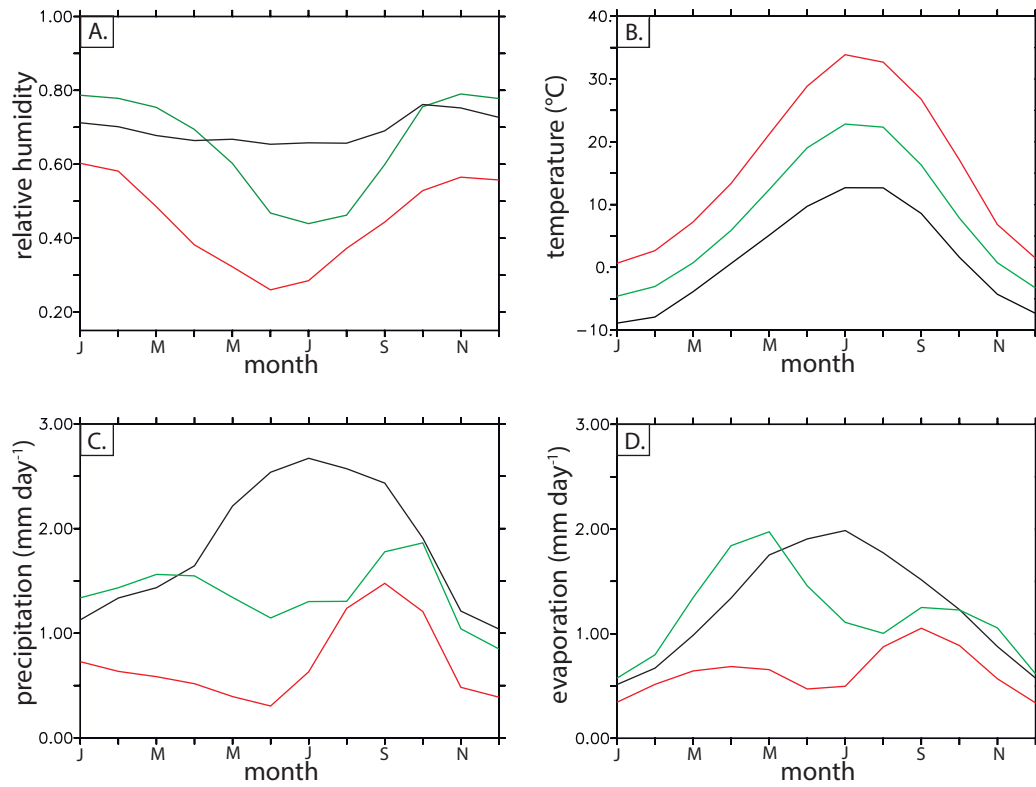


Figure 7. Intraannual variations in (A) low level relative humidity, (B) near-surface temperature, (C) precipitation amount and (D) evaporation amount. All variables are averaged for TP with the altitude over 1500 m. Black colour corresponds to MOD experiment, green - for INT experiment and red - for LOW experiment.

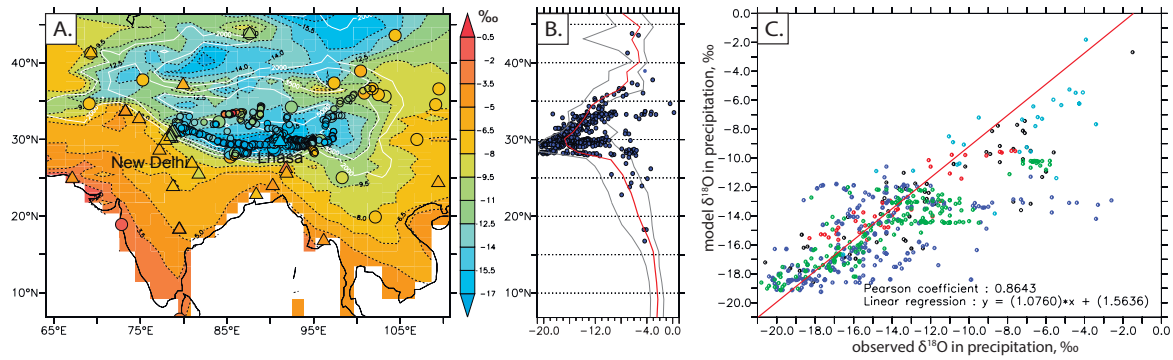


Figure 8. (A) Annual mean  $\delta^{18}\text{O}$  in precipitation simulated by LMDZ-iso for MOD case. Triangles show  $\delta^{18}\text{O}$  in precipitation from GNIP stations, big circles –  $\delta^{18}\text{O}$  in precipitation from Caves et al. (2015) compilation (annual mean and JJA values respectively), small circles represent  $\delta^{18}\text{O}$  in streams, lakes and springs compiled from Quade et al., 2011, Bershaw et al., 2012, Hren et al., 2009. (B) S-N profiles of model simulated  $\delta^{18}\text{O}$  for the MOD case (. Blue points correspond to the same measured data as on panel A. The  $\delta^{18}\text{O}$  profile is averaged between 75° E and 105° E. Grey lines show minimum and maximum values for the selected range of longitudes. (C) Observed vs. modelled  $\delta^{18}\text{O}$  in precipitation. The colour corresponds of circles to the data set: red – Bershaw et al, 2012, blue – Quade et al, 2011, green – Hren et al, 2009, black – Caves et al, 2015, light blue show mean annual data from GNIP stations. Red line shows a linear regression.

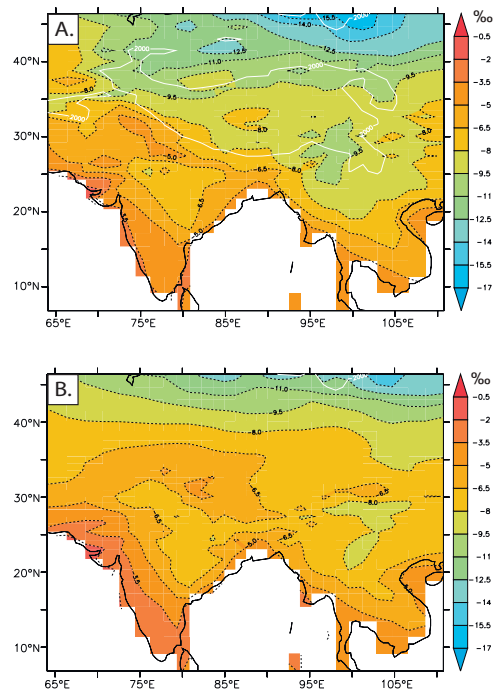


Figure 9. Annual mean  $\delta^{18}\text{O}$  in precipitation simulated by LMDZ-iso for (A) INT case and (B) LOW case



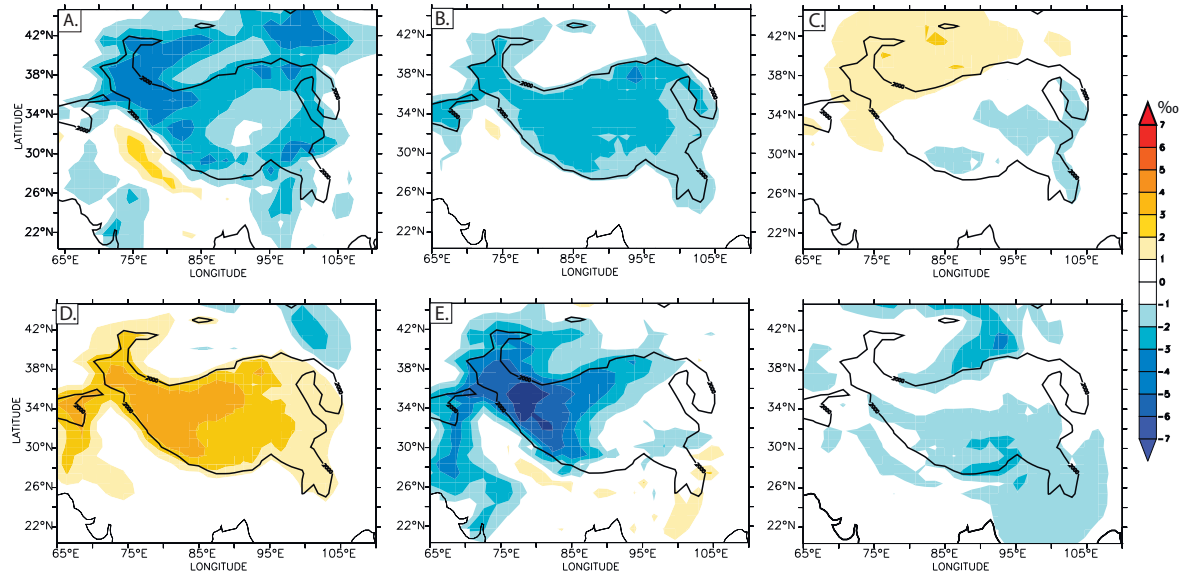


Figure 10. (A) Total isotopic difference between INT and LOW experiments ( $\Delta R_p$ ) and spatial isotopic variations related to: (B) direct effect of topography changes, (C) effect of lapse rate change, associated with non-adiabatic effects, (D) effect of local relative humidity change, (E) effect of changes in post-condensational processes, (F) all other effect (see Table 1)

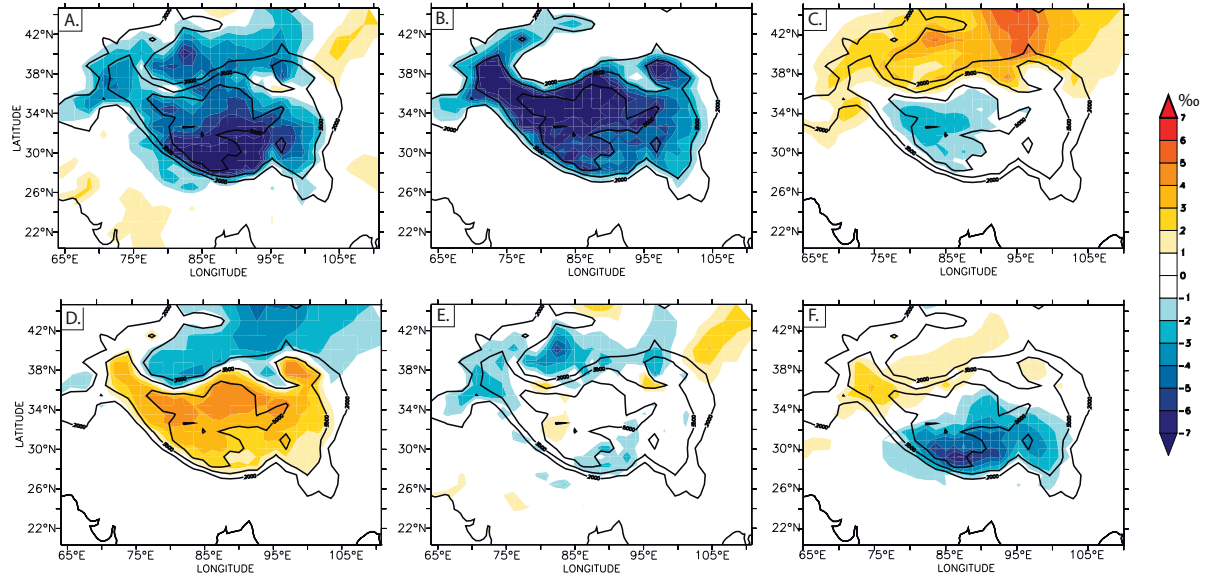


Figure 11. (A) Total isotopic difference between MOD and INT experiments ( $\Delta R_p$ ) and spatial isotopic variations related to: (B) direct effect of topography changes, (C) effect of lapse rate change, associated with non-adiabatic effects, (D) effect of local relative humidity change, (E) effect of changes in post-condensational processes, (F) all other effect (see Table 1)

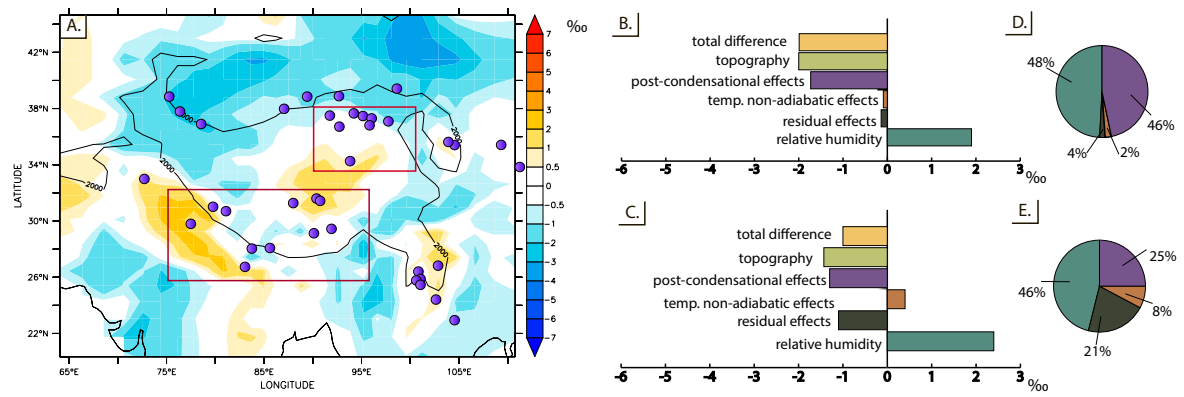


Figure 12. Difference in  $\delta^{18}\text{O}_p$  between INT and LOW experiments that is not related to direct effect of topography changes. Violet points show Cenozoic paleoelevation studies locations (compiled from Caves et al., 2015). Red rectangles show regions for that averaged values decomposed terms are shown: B) Northern region, C) Southern region. Pie diagrams show portion of total isotopic difference related to processes other than topography: D) Northern region, E) Southern region

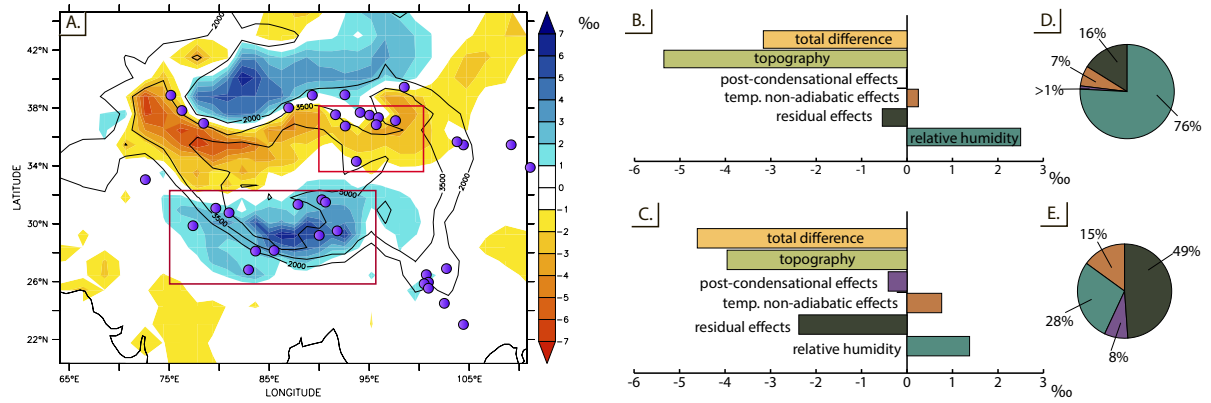


Figure 13. Difference in  $\delta^{18}\text{O}_p$  between MOD and INT experiments that is not related to direct effect of topography changes. Violet points show Cenozoic paleoelevation studies locations (compiled from Caves et al., 2015). Red rectangles show regions for that averaged values decomposed terms are shown: B) Northern region, C) Southern region. Pie diagrams show portion of total isotopic difference related to processes other than topography: D) Northern region, E) Southern region.

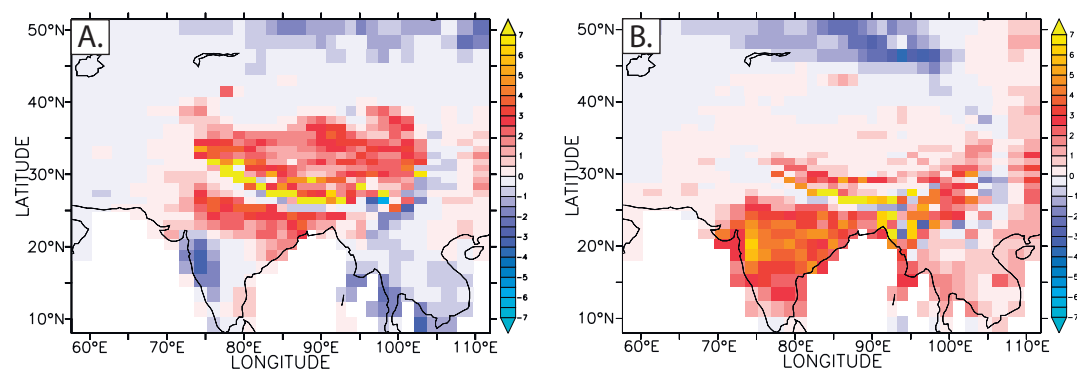


Figure 14. Precipitation change (mm/day) for A) MOD-INT B) INT-LOW cases